

Cooperative Target Tracking using Mobile Robots

Ph.D. Dissertation Proposal
submitted by

Boyoon Jung

February 2004

Guidance Committee

Gaurav S. Sukhatme (Chairperson)
Maja J. Matarić
Milind Tambe
Isaac Cohen
Kwan Min Lee (Outside Member)

Abstract

We study the problem of multiple target tracking using multiple mobile robots. Our approach is to divide the cooperative multi-target tracking problem into two sub-problems: target tracking using a single mobile robot and on-line motion strategy design for multi-robot coordination.

For single robot-based tracking, we address two key challenges: how to separate the ego-motion of the robot from the motions of external objects, and how to compensate this ego-motion to detect and track moving objects robustly. An ego-motion compensation method using salient feature tracking is described, and the design of a probabilistic filter to handle the noise and uncertainty of sensor inputs is presented. The proposed method is implemented and tested in various outdoor environments using three different robot platforms: a robotic helicopter, a Segway RMP, and a Pioneer2 AT, which have unique ego-motion characteristics.

For multi-robot coordination, we propose an algorithm based on treating the densities of robots and targets as properties of the environment in which they are embedded. By suitably manipulating these densities a control law for each robot is proposed. We term our approach *Region-based*, and describe and validate it through an example. We observe that the general approach can be significantly improved in the special case where the topology of the environment is known in advance. We derive a specialized version of the control law for this case; the resulting algorithm is called the *Topological Region-Based Approach*. We also give the formulation of the solution in the unstructured case, termed the *Grid Region-Based Approach*. These coordination approaches have been implemented in simulation, and in real robot systems. Experiments indicate that our treatment of the coordination problem based on environmental characteristics is effective and efficient.

There are four additional topics we plan to address for the final thesis. First, sensor fusion techniques will be studied for target position estimation in 3D space. The current single-robot tracker integrates laser range scans into the estimation system by simply projecting the scans into the 2D image space, which causes poor estimation results when a robot turns at high velocity. Second, the stability properties of the *Region-based Approach* will be analyzed theoretically and through simulations. The system's behavior in response to static or oscillating target motions will be studied. Third, the performance of the *Grid Region-based Approach* will be tested and

characterized through intensive simulations with various configurations in order to investigate the effect of environmental structure, broken inter-robot communication links, and increased target population. Finally, all system components will be integrated, and tracking experiments in an outdoor setting using multiple robots will be performed to test the robustness of the entire system.

Contents

Abstract	ii
List Of Figures	vii
List Of Tables	ix
1 Introduction	1
1.1 Problem Statement	2
1.2 Expected Contributions	3
1.3 Proposal Outline	5
2 A Taxonomy and Summary of Related Work	6
2.1 Variations on Problem Definition	6
2.1.1 The Number of Trackers versus the Number of Targets	6
2.1.2 Ratio of the number of targets to the number of trackers	8
2.1.3 Mobility of Trackers	9
2.1.4 Complexity of Environments	10
2.1.5 Prior Knowledge of Target Motion	11
2.1.6 Type of Cooperation	12
2.1.7 Coordination of Multiple Trackers	13
2.2 Variations on Evaluation Criteria	13
2.3 Problem Classification	14
3 Moving Object Tracker	16
3.1 Problem Statement Revisited	16
3.2 Related Work	18
3.3 Ego-motion Compensation	19
3.3.1 Feature Selection and Tracking	19
3.3.2 Transformation Estimation	21
3.3.3 Frame Differencing	23
3.4 Motion Detection in 2D Image Space	23
3.4.1 Particle Filter Design	25
3.4.2 Particle Clustering	26
3.5 Position Estimation in 3D Space	27
3.6 Experiments	29

3.6.1	Experimental Setup	29
3.6.2	Experimental Results	30
3.7	Discussion	35
4	Cooperative Multi-Target Tracking	36
4.1	Problem Statement Revisited	36
4.2	Related Work	37
4.3	Region-based Approach	38
4.3.1	Relative Density Estimates as Attributes of Space	39
4.3.2	Urgency Distribution and Utility	43
4.3.3	Distributed Motion Strategy	44
4.4	Grid Region-Based Approach	46
4.4.1	Virtual Region Representation and Density Estimates	46
4.4.2	Estimation of the Utility Distribution	47
4.4.3	Motion Strategy for Cooperative Target Tracking	48
4.5	Topological Region-based Approach	50
4.5.1	Density Estimates on a Topological Map	50
4.5.2	The Coarse Deployment Strategy	51
4.5.3	Target Tracking within a Region	52
4.6	Discussion	53
5	Experiments in Structured Environments	54
5.1	System Design and Implementation	54
5.1.1	The Motor Actuation Layer	54
5.1.2	The Target Tracking Layer	56
5.1.3	Monitoring Layer	56
5.2	Experimental Setup	57
5.2.1	Target Modeling	58
5.2.2	Environment Complexity	58
5.2.3	Experiment Design	60
5.2.3.1	Region-based versus Local-following Strategy	60
5.2.3.2	Robot Density versus Visibility	61
5.2.3.3	Mobile Robots versus Embedded Sensors	61
5.3	Experimental Results	62
5.3.1	Region-based versus Local-following Strategy	62
5.3.2	Robot Density versus Visibility	62
5.3.3	Mobile Robots versus Embedded Sensors	62
5.4	Discussion	65
5.4.1	Region-based versus Local-following Strategy	65
5.4.2	Robot Density versus Visibility	66
5.4.3	Mobile Robots versus Embedded Sensors	67
5.4.4	Summary	67

6	Experiments in Unstructured Environments	69
6.1	System Design and Implementation	69
6.1.1	Motion Tracker	69
6.1.2	Localization	69
6.1.3	Cooperative Motion Planning	71
6.1.4	Navigation	72
6.2	Experimental Setup	72
6.3	Experimental Results	73
6.4	Discussion	74
7	Conclusion and Future Work	77
7.1	Research Plan	78
	Reference List	80
	Appendix A	
	List of Publications	89
A.1	Refereed Journal Papers	89
A.2	Refereed Conference Papers	89
A.3	Unrefereed Technical Reports	90
	Appendix B	
	Extension: Visibility Maximization	91

List Of Figures

1.1	Cooperation among multiple robots	3
1.2	Multiple Target Tracking using Multiple Robots	4
2.1	Research in target tracking problem	15
3.1	Multiple Target Tracking using a Single Robot	17
3.2	Processing sequence for moving object tracking from a mobile robot	18
3.3	Salient features selected for tracking	20
3.4	Feature tracking	21
3.5	Outlier feature detection	22
3.6	Image Transformation	24
3.7	Results of frame differencing	24
3.8	Particle filter tracking	27
3.9	Projection of laser scans onto the image coordinates	28
3.10	Projected laser scans	29
3.11	Robot platforms for experiments	30
3.12	Snapshots of particle filter tracking a moving object: from Robotic helicopter	31
3.13	Snapshots of particle filter tracking a moving object: from Segway RMP	32
3.14	Snapshots of particle filter tracking a moving object: from Pioneer2 AT	32
3.15	Performance evaluation: tracking from Robotic helicopter	33
3.16	Performance evaluation: tracking from Segway RMP	33
3.17	Performance evaluation: tracking from Pioneer2 AT	34
4.1	Positions of mobile robots and targets in a bounded environment	39
4.2	Robot distribution model	40
4.3	Target distribution model	41
4.4	Region models for density computation	41
4.5	Robot density distribution	42
4.6	Target density distribution	43
4.7	Urgency distribution	44

4.8	Example of a cost function	45
4.9	Utility distribution	45
4.10	Parameterized virtual region	47
4.11	Snapshot of the utility distribution	49
4.12	Example of a topological map	50
4.13	Following targets within a region	53
5.1	Behavior-based robot control architecture	55
5.2	Configurations for robots and targets	57
5.3	System architecture for targets	58
5.4	The simulation environments	59
5.5	Environment for real-robot experiments	62
5.6	Simulation results comparing the performance of the two strategies	63
5.7	Performance with visibility maximization	64
5.8	Performance of the real-robot system	64
5.9	Tracking examples	68
6.1	System architecture for <i>Grid Region-based Approach</i>	70
6.2	Robot localization using Kalman filters	71
6.3	Navigation using the VFH+ algorithm	73
6.4	Virtual region selection behavior	74
6.5	Region-switching behavior	76
B.1	Coverage computation	91
B.2	Visibility maximization method relying on local sensing	92

List Of Tables

3.1	Adaptive Particle Filter Algorithm	26
3.2	Expectation-Maximization Algorithm for Particle Clustering	28
3.3	Performance of moving object detection algorithm	34
5.1	Complexity of the environments as a function of number of targets	60
5.2	Significance values from T-test as a function of number of targets and environment characteristic	65
5.3	Significance values from T-test as a function of number of targets and different strategies	66
7.1	Timetable for future work	79

Chapter 1

Introduction

The target tracking problem is to estimate the state of a target¹ based on inaccurate measurements from sensors. The estimation process contains many uncertainties; for example, the measurements are corrupted by noise, the origin of the measurements are unauthenticated, the motion of the target is unknown, etc. The roots of the target tracking problem go back to World War II, when automated systems to control anti-aircraft guns were developed, and algorithms were designed to track aircraft using RADAR and predict their future positions. Present day applications of target tracking algorithms range from automated surveillance to security systems, which require the capability of tracking the positions of multiple targets (*eg.* people in a building) autonomously and effectively.

The target tracking problem has been studied in diverse research areas with many applications in mind. Traditionally, the signal processing community (Bar-Shalom, 1992; Biernson, 1990; Blackman, 1986; Bogler, 1990; Kolawole, 2002; Siouris et al., 1997) has designed probabilistic filters to track missiles or vehicles using RADAR for mainly military purposes. The computer vision community (Behrad et al., 2001; Cohen and Medioni, 1999; Foresti and Micheloni, 2003; Kang et al., 2002; Koyasu et al., 2001; Lipton et al., 1998; Murray and Basu, 1994) has developed algorithms to track visual targets using camera(s), and the sensor network community (Guibas, 2002; Horling et al., 2001; Li et al., 2002; Liu et al., 2002; Moore et al., 2003; Zhao et al., 2002) has utilized deployed sensors to monitor moving objects in an environment.

We are interested in tracking targets using mobile robots as the tracking devices. Using a group of mobile robots for target tracking is beneficial because:

1. A mobile robot can cover a wide area over time, which means the number of sensors required for tracking can be kept small.

¹In this thesis, we assume that a target is a moving object and its state is its location.

2. A mobile robot can re-position itself in response to the movement of the targets for efficient tracking.

When the number of targets is much bigger than the number of sensors available or when sensors cannot be deployed in advance, the mobility of sensors become indispensable. For surveillance and security applications, multiple robots can be used for efficient monitoring; this requires a coordinated motion strategy for cooperative tracking.

The motion tracking and estimation of moving objects in the vicinity of a mobile robot is also a fundamental capability for safe navigation. Populated environments are challenging to contemporary mobile robots. One of the main reasons is the presence of dynamic objects, whose motions are diverse (*eg.* due to pedestrians, bicycles, automobiles, etc). Since some objects move faster than the robot, motion detection and estimation for potential collision avoidance are the most fundamental skills that a robot needs to function effectively in dynamic environments. Needless to say, target tracking is a key enabler for robust motion estimation.

This thesis addresses the development of a multiple target tracking system using multiple mobile robots. Intuitively tracking performance can be improved by exploiting multiple robots, and cooperation among the robots is the key point to take advantage of the multi-robot system. There are two expected improvements attributable to multi-robot cooperation. The uncertainty of target position estimation can be reduced by combining measurements from multiple robots (Spletzer and Taylor, 2003; Stroupe et al., 2001). In this case, the motion strategy of each robot is to minimize the redundant measurement uncertainty; for example, when the horizontal and vertical uncertainties of a single-robot measurement are different, two robots can minimize the total estimation error by positioning themselves so that their headings are orthogonal to each other (Figure 1.1 (a)). As the other possible improvement, the total number of tracked targets over time can be maximized by distributing robots properly and allocating targets to a robot in the best position (Jung and Sukhatme, 2002; Parker, 1999; Wergler and Matarić, 2000). The motion strategy of robots for this case is to minimize the redundant target allocation; for example, each target would be allocated to a robot in the best position according to the tracking range, which stops multiple robots from tracking the same target. Both cases require that the amount of exchanged information among robots should be minimized, and the collective data should be simple enough to be processed in real-time. We focus on the latter type of cooperation.

1.1 Problem Statement

The multiple target tracking problem using multiple mobile robots is defined as follows.

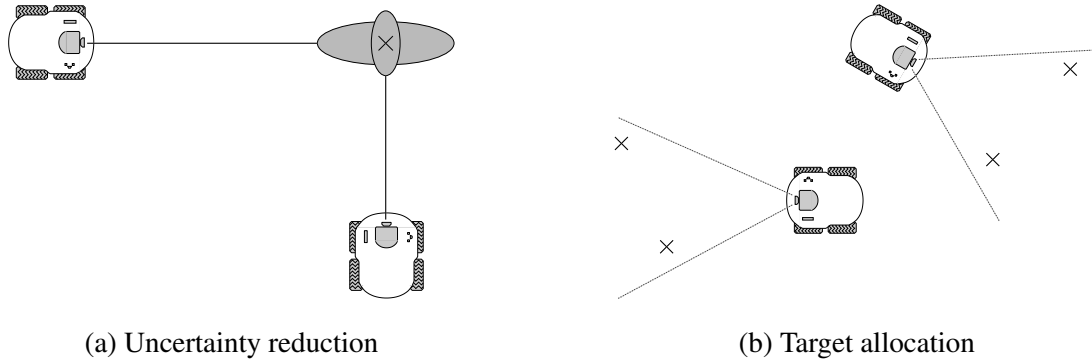


Figure 1.1: Cooperation among multiple robots: The uncertainty of estimation can be reduced by combining multiple measurements, or the total number of tracked targets can be maximized by allocating each target to a robot in the best pose.

Input Multiple mobile robots and multiple targets in an environment

Output Positions of detected targets in a global coordinate system

Goal To maximize the number of tracked targets over time

Restriction No prior knowledge of the number of robots, the number of targets, or a target motion model

A decomposition of the problem is shown in Figure 1.2. The system consists of M robots and N targets, and the available measurements are sensor data for robot localization (*eg.* GPS, IMU, and odometry) and target detection and tracking (*eg.* camera and laser rangefinder). Since the multi-robot system has no control over target motions, the only factor to maximize the number of tracked targets is each robot's motion control. Based on the current poses of mobile robots and the current positions of targets, each robot infers the best new position to move toward, in order to maximize the number of tracked targets over time.

Our design goal is to develop a hierarchical system by decoupling the (low-level) target-tracking algorithm and the (high-level) cooperation strategy. The low-level tracking algorithm focuses on the single-robot, multiple-target problem so that an individual robot performs robust target tracking. On top of the low-level capability, an on-line, coordinated motion strategy is developed for robot positioning in distributed manner, resulting in a solution to the multi-robot tracking problem.

1.2 Expected Contributions

Here we outline the significant contributions presented in the thesis.

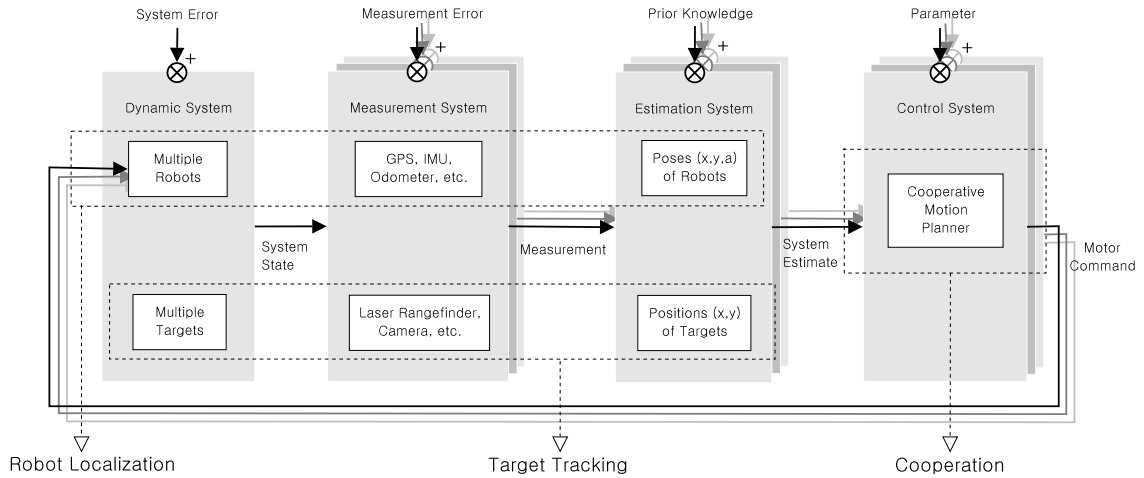


Figure 1.2: Multiple Target Tracking using Multiple Robots: The problem can be decomposed into three sub-problems: robot localization, target tracking, and cooperation.

1. The taxonomy of the target tracking problem, presented in Chapter 2.

The target tracking problem has been studied by diverse research communities in different perspectives for various applications. We provide a taxonomy that classifies previous research according to the variants of the problem definitions and evaluation criteria. For each cluster within this classification, the main research issues and related literature are described.

2. Moving object tracker design and its experimental evaluation, presented in Chapter 3.

We address two key challenges for single robot-based moving object tracking: how to separate the ego-motion of the robot from the motions of external objects, and how to compensate this ego-motion to detect and track moving objects. An ego-motion compensation method using salient feature tracking is described, and the design of a probabilistic filter to handle the noise and uncertainty of sensor inputs is presented. The proposed method is implemented and tested in various outdoor environments using three different robot platforms, which have unique ego-motion characteristics.

3. New mechanism for cooperative tracking using multiple robots, presented in Chapter 4.

We propose an algorithm for multi-robot coordination with applications to multiple target tracking. The proposed algorithm treats the densities of robots and targets as properties of the environment in which they are embedded, and a control law for each robot is generated by suitably manipulating these densities. Since the proposed mechanism is *distributed* and

expandable, it can be applied for various sensor configurations. For example, a *heterogeneous* sensor network can adopt the mechanism with minimal modification, and sensors can be added to (or subtracted from) a tracking network on the fly without stopping operation. Experiments indicate that our treatment of the coordination problem based on environmental characteristics is effective and efficient.

4. Introduction of an *environmental complexity metric* for tracking performance analysis, presented in Section 5.2.2.

In structured environments, we exploit the topology of the environment to optimize tracking, so the structure and complexity of an environment has an indirect effect on the overall tracking performance. A method to measure the complexity of an environment is presented, and the influence of environmental structure on tracking is experimentally verified.

5. Demonstration of possible improvement by constructing a sensor network using mobile and stationary sensors, presented in Section 5.2.3.3.

Both mobile and stationary trackers have their own advantages. For example, a mobile tracker can cover wider area over time, and can adapt to targets' movement patterns. On the other hand, a stationary tracker can be installed at the best position depending on the environments, and cause less interference. We demonstrate that performance improvement is expected by constructing a sensor network with both kinds of trackers.

1.3 Proposal Outline

This thesis proposal is organized as follows. Chapter 2 provides a summary of previous research. The tracking problem has been studied in diverse areas; we categorize related work based on problem definition and evaluation criteria. Chapter 3 describes our approach for a moving-object tracker using a single robot. There are two independent motions involved: motions of moving objects and the ego-motion of the robot. The ego-motion is compensated for motion detection and tracking. Chapter 4 presents our cooperation mechanism for multiple target tracking using multiple mobile robots. The general idea is described first, and two implementations for different environments are described. In Chapter 5 the experimental results from a structured indoor environment are discussed; the experimental results for an unstructured outdoor environment are analyzed in Chapter 6. Finally, the current status and plans for thesis completion are discussed in Chapter 7.

Chapter 2

A Taxonomy and Summary of Related Work

The target tracking problem has been studied by various research groups from different points of view. Even though the basic concept of estimating the position of an interesting object remains same, the detailed problem definition or approaches are different. As a way of differentiating our work from previous research, we present a taxonomy that classifies tracking research according to the various problem definitions and evaluation criteria.

2.1 Variations on Problem Definition

The target tracking problems can be classified along multi-dimensions. There are several natural dimensions, for example, the number of trackers¹, the number of targets, the mobility of trackers, etc.

2.1.1 The Number of Trackers versus the Number of Targets

The most natural classification axis is the number of trackers, and the axis can be divided into 'single' or 'multiple' based on whether cooperation among trackers is planned or not. Even when there are multiple trackers involved in a system, we consider it as a single tracker problem if there is no cooperation among the trackers. Another obvious axis is the number of targets, which affects the complexity of data association problem² or multi-tracker cooperation strategy.

¹In some papers (Bar-Shalom, 1990) the general term, *sensor*, is used to describe an elemental tracking device. The terminology is appropriate when each sensor returns a partial or full state measurement of a target. For example, a RADAR sensor returns a 2 dimensional position information of a target, and the sensor is a tracker. However, it becomes confusing when there are sensors in the system whose measurements provide no information of target state. For example, when a mobile robot equipped with a camera and a GPS sensor is used for a target tracking in the global coordinate system, the GPS sensor is not a tracker because it measures only the robot state. In this case, a mobile robot is a tracker. Therefore, we use the collective term, *tracker* to indicate an elemental tracking device.

²The data association problem is to find the origin of measurements. Even for a single target case, the data association problem (*eg.* does a measurement originate from a target or noise?) needs to be solved, but when there are

A tracking problem can be classified under one of the following four categories according to the combination of these two axes.

Single Tracker Single Target (STST) A single tracker is used to track a single target. Most work in this category focuses on signal processing techniques for target detection, probabilistic filter design to filter out noisy measurements, and failure recovery. The Kalman filter (Bar-Shalom and Fortmann, 1988; Biernson, 1990; Bogler, 1990) and the particle filter (Gustafsson et al., 2002; Isard and Blake, 1998) have been applied to the single target tracking problem successfully. Liu and Fu (2001) proposed the Probabilistic Data Association (PDA) filter to achieve successful tracking in cluttered environments. Chung and Yang (1995); Coué and Bessiére (2001) presented visual servoing techniques to track a target, and Fabiani et al. (2002); LaValle et al. (1997); Murrieta-Cid et al. (2002) introduced the motion strategy of a mobile robot maintaining visibility of a moving target in a cluttered workspace. Many efforts (Behrad et al., 2001; Foresti and Micheloni, 2003; Murray and Basu, 1994; Nordlund and Uhlin, 1996; Yilmaz et al., 2001) to detect and track a visual target using a single camera come from the computer vision community.

Single Tracker Multiple Targets (STMT) A single tracker is used to track multiple targets. The research in this category focuses on data association and target identification. Cox and Hingorani (1996); Danchick and Newnam (1993); Reid (1979) presented the Multiple Hypothesis Tracking (MHT) algorithm and its application to visual tracking. Bar-Shalom and Fortmann (1988); Fortmann et al. (1983) introduced the Joint Probabilistic Data Association Filter (JPDAF) that computes the probabilities of measurement association to the multiple targets, and Frank (2003); Schultz et al. (2001) extended it using a sample-based method. Carine Hue and Pérez (2002); Herman (2002); Meier and Ade (1999); Montemerlo et al. (2002); Orton and Fitzgerald (2002) demonstrated how the particle filter can be exploited for the data association problem. Cohen and Medioni (1999) utilized a graph representation to store template information of moving objects, and solved the data association problem by searching an optimal path in the graph.

Multiple Trackers Single Target (MTST) A single target is tracked by multiple trackers. The main issue in this category is how to combine multiple measurements from multiple trackers to improve the estimation accuracy. Dana (1990); Kang et al. (2002) described registration procedure that projects sensory data from multiple sources into a common global

multiple targets involved, the uncertainty of measurement origin increases drastically because a measurement could originate from one of many targets, or from noisy input.

coordinate system, and Brooks and Williams (2003); Maybeck et al. (1994); Wilhelm et al. (2002) presented target-tracking systems that fuse two estimates from heterogeneous trackers for better accuracy or robustness. Stroupe et al. (2001) demonstrated that the accuracy of ball tracking was improved by combining data from multiple robots, and Spletzer and Taylor (2003) presented a control strategy to move multiple robots to the optimal positions so that the estimation uncertainty of target position is minimized. Most target tracking research using a sensor network (Horling et al., 2001; Li et al., 2002; Liu et al., 2002; Moore et al., 2003; Zhao et al., 2002) falls under this category.

Multiple Trackers Multiple Targets (MTMT) Multiple trackers are used to track multiple targets cooperatively. The research focuses on how to combine multiple measurements and solve the association problem at the same time, how to position trackers to track more targets, or how many trackers are required for a given environment and targets. Blackman (1990); Chong et al. (1990) outlined the issues and the methods related to the fusion of multiple sensor data or the association of multiple tracks. Gerkey and Matarić (2001); Jung and Sukhatme (2002); Parker (1999); Wergler and Matarić (2000) proposed various multi-robot motion strategies to maximize the number of targets over time. Guibas et al. (1997); Yamashita et al. (1997) introduced a few theoretical bounds on how many trackers are necessary and sufficient to search well-defined environments (*eg.* polygonal region or simply-connected free space).

This thesis presents a solution for the MTMT problem when trackers are mobile robots. In contrast to other approaches, the presented solution decouples the low-level tracking and the high-level cooperation for simplicity. Note that the low-level tracking is simply the STMT problem.

2.1.2 Ratio of the number of targets to the number of trackers

There is another classification axis related to the number of trackers and targets, the ratio r of the number of targets to the number of trackers. For the MTST and MTMT problem, this ratio is one of the characteristics that influences the solution approaches.

$r \ll 1.0$ The extreme case in this category is a sensor network (Horling et al., 2001; Li et al., 2002; Liu et al., 2002; Moore et al., 2003; Zhao et al., 2002), which assumes a very large number of sensors spread in an environment and few objects in it. Each sensor has limited capability and its measurement contains high uncertainty (*eg.* distant measurement only or existence in a certain range only), and the tracking is performed by triangulating or

overlapping multiple measurements. Also, most MTST problems (Dana, 1990; Spletzer and Taylor, 2003; Stroupe et al., 2001) fall under this category.

$r \approx 1.0$ When there are enough trackers available to track all targets, the tracking problem can be treated as a task allocation problem (Gerkey and Matarić, 2001; Parker, 1999; Werger and Matarić, 2000). Based on the current positions of trackers and targets, each target is allocated to each tracker to improve overall tracking performance.

$r \gg 1.0$ When the number of trackers is not big enough to track all targets (Jung and Sukhatme, 2002), trackers are allocated according to spatial density rather than to targets themselves. Research on how to characterize space based on target positions and how to position trackers based on these characteristics are the main issues.

This thesis focuses the third case when the number of targets is much bigger than the number of trackers, which implies cooperation among trackers is indispensable.

2.1.3 Mobility of Trackers

Perhaps the most interesting axis for roboticists is the mobility of trackers. Based on the degree of possible tracker motions, we classify the tracking problem as stationary, pan/tilt/zoom, planar, and unrestricted.

Stationary Since there is no motion control involved in this category, most work focuses on reliable perception. Biernson (1990); Bogler (1990); Kolawole (2002) presented RADAR-based trackers, and Haritaoglu et al. (1998); Kang et al. (2002); Lipton et al. (1998) described visual target trackers using a single or multiple stationary cameras. Sonars (Fortmann et al., 1983) and laser rangefinders (Brooks and Williams, 2003; Fod et al., 2002) are also utilized to track targets.

Pan/Tilt/Zoom The Pan/Tilt/Zoom motion does not allow the tracker to move. Such trackers extend the field and range of sensing, but have intrinsic limitations caused by the fixed center position. Foresti and Micheloni (2003); Murray and Basu (1994) describe a target tracking system using a single PTZ camera, and Kang et al. (2003); Stillman et al. (1998) presented a heterogeneous tracking system that consists of a stationary camera and a PTZ camera.

Planar The motion of a tracker is planar. For example, a pointing-down camera mounted on an airplane flying at a constant altitude (Cohen and Medioni, 1999; Gustafsson et al., 2002)

was used to construct a background model by mosaicking input images, or a mobile robot with a planar scan device (*eg.* a sonar array or a SICK laser rangefinder) moving on a flat surface (Kluge et al., 2001; Montemerlo et al., 2002; Schultz et al., 2001) can build a 2D map of an environment. In both cases, moving targets can be detected by comparing measurements to the planar model of the environment.

Unrestricted There is no restriction on the tracker motion. A camera mounted on a mobile robot (Chung and Yang, 1995; Coué and Bessiére, 2001; Jung and Sukhatme, 2004; Nordlund and Uhlin, 1996) and a forward-looking infrared (FLIR) sensor attached to an airborne platform (Braga-Neto and Goutsias, 1999; Maybeck et al., 1994; Yilmaz et al., 2001) are examples.

The target tracker described in the thesis is a mobile robot with a single camera and a laser rangefinder. Three different robot platforms are utilized to test the robustness of our tracking algorithm. The case of using the robot helicopter falls under the third category and the other two cases fall under the fourth category. The detailed motion characteristics of the platforms are explained in Section 3.6.1.

2.1.4 Complexity of Environments

The complexity of the environment is an important factor for system design, especially when trackers are mobile since the interaction between trackers and the environment should be taken into account. Even when trackers are stationary, a tracking system should be able to recover from lost tracking due to occlusion caused by the structure of an environment.

Empty Space Brooks and Williams (2003); Parker (1999); Spletzer and Taylor (2003); Werger and Matarić (2000) make the open space assumption and focus only on the interaction among trackers and targets. Even though the assumption is not made explicitly, some works (Murray and Basu, 1994; Nordlund and Uhlin, 1996; Wilhelm et al., 2002) do not take occlusion into account for their system design, then we categorize them in this class.

Structured Space When the environment is structured (*eg.* office-type, indoor environment), a tracking system can actively exploit the structure of the environment for target detection (Meier and Ade, 1999; Montemerlo et al., 2002; Schultz et al., 2001) or tracker motion planning (Jung and Sukhatme, 2002; Murrieta-Cid et al., 2002). Also, Behrad et al. (2001); van Leeuwen and Groen (2002) presented front-car tracking systems on a paved road, and those works fall under this category since they utilized the characteristics of parallel lanes.

Unstructured Space When an environment is cluttered the environment is classified as *unstructured*. Most works using probabilistic filters (Bar-Shalom and Fortmann, 1988; Houles and Bar-Shalom, 1989; Orton and Fitzgerald, 2002; Reid, 1979) treat occlusion caused by environmental structure as uncertainty in sensor measurements. Coué and Bessiére (2001); Fabiani et al. (2002); LaValle et al. (1997); Spletzer and Taylor (2003) presented motion strategies for mobile robot-based trackers that minimize the loss of tracking performance in cluttered environments.

The cooperative tracking algorithm presented in this thesis is implemented with two different level of discretization. The first case described in Section 4.4 assumes an unstructured space, and treats the environmental structure as an obstacles. The second case described in Section 4.5 assumes a structured space and actively takes advantage of the environmental structure for multi-robot coordination. The individual tracking algorithm in Chapter 3 assumes and runs in unstructured environments.

2.1.5 Prior Knowledge of Target Motion

Prior knowledge of targets' motion is an important determinant since tracking solutions may be different depending on the motions of targets (*eg.* random vs. predictable).

Deterministic The most well-known example in this category is the traditional missile tracking problem (Kirubarajan et al., 2001; Siouris et al., 1997; Song et al., 1990). Since the trajectory of a missile is governed by physics, future position can be inferred from a current state. For example, the missile approach warning system (MAWS) (Difilippo and Campbell, 1995) detects approaching missiles with enough warning time, and uses a deterministic model of the target to compute the impact time and position. Spletzer and Taylor (2003) discusses a multi-robot system that tracks an aerial target, whose motion was deterministic.

Probabilistic The prior knowledge of targets' motion can be modeled with random variables. For example, the motion of a maneuvering aircraft (Cooperman, 2002) or of a tactical ballistic missile (Vacher et al., 1992) cannot be captured using a single model. The interacting multiple model (IMM) methods (Bar-Shalom et al., 1989; Blom and Bar-Shalom, 1988; Houles and Bar-Shalom, 1989; Mazor et al., 1998) has been applied to those type of target tracking problems; multiple dynamic models and their transition probabilities are designed *a priori*, and a tracking system estimates not only the kinematic components but also the

best suitable model. Ikoma et al. (2002); McGinnity and Irwin (2001) presented sample-based methods for model switching, and LaValle et al. (1997) computed optimal, numerical solutions for a robot motion strategy when the target is predictable.

Unknown For real-world applications, the motion model of a target is often unavailable. In such cases, there is no priori information about target movements, simple constant motion models are utilized (Fod et al., 2002; Jung and Sukhatme, 2004; Kang et al., 2003; Koyasu et al., 2001; Spletzer and Taylor, 2003). Montemerlo et al. (2002) assumed the Brownian motion for a person's typical movements to avoid estimating the velocity or acceleration of a person.

The targets we attempt to track are any moving objects in the vicinity of a robot, and the motions of the objects are diverse (*eg.* a person, a mobile robot, an automobile, etc.). Since there is no assumption about the target variety, there is no prior information of target motions available. We utilize a constant velocity model for robust tracking.

2.1.6 Type of Cooperation

For MTST and MTMT problems, cooperation among trackers is essential to improve tracking performance, and two different types of improvement are expected:

Uncertainty Reduction The uncertainty of target position estimation can be reduced by combining measurements from multiple trackers. Kang et al. (2002); Stillman et al. (1998) demonstrated how the estimation error due to occlusion can be eliminated by using multiple cameras, and Brooks and Williams (2003); Wilhelm et al. (2002) presented tracking systems that combines a visual tracker and a range tracker for better estimation. Spletzer and Taylor (2003); Stroupe et al. (2001) described multi-robot systems whose motion strategy is to minimize the total estimation error.

Target Allocation The number of tracked targets over time can be maximized by distributing trackers properly and allocating each target to a single tracker in the best position. Jung and Sukhatme (2002); Parker (1999); Werger and Matarić (2000) presented cooperative motion strategies for multi-robot systems, which attempt to minimize redundant target allocation. In the ideal case every target is allocated to a single robot and every robot can track all targets allocated to itself.

The goal of our research is to develop a control algorithm that deploys mobile robots according to the target distribution so that the overall tracking performance is improved, which requires the second type of cooperation.

2.1.7 Coordination of Multiple Trackers

When multiple trackers are used for target tracking and some of them have autonomy (*eg.* a target tracking system using multiple mobile robots), a coordination strategy should be designed so that the effect of cooperation can be maximized. The coordination strategy can be classified according to whether or not the behavior of a tracker can be modified directly by other trackers' decision.

Explicit One tracker can modify the behaviors of other trackers by explicit communication.

Werger and Matarić (2000) presented the *Broadcast of Local Eligibility (BLE)* technique; if a particular robot thinks it is best suited to track a specified target, it stops other robots from tracking the target by broadcasting inhibition signals over the network. Gerkey and Matarić (2001) demonstrated that the target tracking problem can be solved using a principled publish/subscribe messaging model; the best capable robot is assigned to each tracking task using a one-round auction.

Implicit All trackers make their own decision independently based on their best knowledge acquired by exchanging information or observing others. Parker (1999) presented *ALLIANCE* architecture to achieve target-assignment. If a robot was not able to track an assigned target for a while, it would give up tracking the target. If a robot observes a target that has not been tracked for a while, the robot would assign the target to itself. These behaviors are achieved through the interaction of the *motivational behavior*; there is no explicit hand-over mechanism.

There is no inhibition signal or two-way negotiation in our coordination method. Robots share tracking information by broadcasting them, but the final decision is made independently, which puts our work under the second category.

2.2 Variations on Evaluation Criteria

Tracking evaluation criteria vary from application to application; for example, a missile defence system requires high accuracy of tracking results, but a surveillance system may prefer a tracking system that can cover a wide area. Therefore, evaluation criteria are an important factor for tracking system design.

Tracking Accuracy The most popular evaluation criterion is tracking accuracy. Since the target tracking problem is to estimate the state of a target from noisy measurements, it is key to filter out noise from measurements (Bar-Shalom and Fortmann, 1988; Biernson, 1990;

Bogler, 1990; Gustafsson et al., 2002; Isard and Blake, 1998), how to combine measurements from multiple sources (Brooks and Williams, 2003; Dana, 1990; Kang et al., 2002; Maybeck et al., 1994; Wilhelm et al., 2002), or how to distribute trackers to achieve better accuracy (Spletzer and Taylor, 2003).

Collective Time Another popular evaluation criteria is the total collective time that targets are tracked, which is proper to evaluate motion strategies of mobile tracking system. Especially when the number of targets are bigger than the number of trackers and it is impossible to track all targets all the time, the goal of a tracking system is often to maximize the number of tracked targets over time (Jung and Sukhatme, 2002; Parker, 1999; Werger and Matarić, 2000).

Energy Efficiency For target tracking using a sensor network, power consumed in transmitting or receiving messages for cooperation is a reasonable norm (Moore et al., 2003; Xu and Lee, 2003; Zhang and Cao, 2004) since energy is the most limited resource of wireless sensor nodes.

Travel Distance When trackers are mobile and the goal of the system is to track targets in bounded environments, the total travel distance of a tracker can be used for performance evaluation assuming a tracker is always able to track targets.

Escape Time When the motion of a target is evasive, escape time is an interesting evaluation criterion assuming targets eventually escape from all trackers. Trackers are mobile for this criterion.

The purpose of the low-level target tracking algorithm in Chapter 3 is to locate the target positions using a camera and a laser rangefinder, and the accuracy of the tracking results was analyzed in Section 3.6. On the other hand, the goal of the multi-robot system in Chapter 4 is to maximize the number of tracked targets over time by re-positioning themselves, and the total collective time was discussed in Chapter 5.

2.3 Problem Classification

The taxonomic axes proposed in the previous sections can be used to classify related research or to distinguish one approach from others. As an example, target tracking research performed by different communities can be categorized according to tracker mobility and the ratio of the number of trackers to the number of targets as shown in Figure 2.1. The proposed approach in

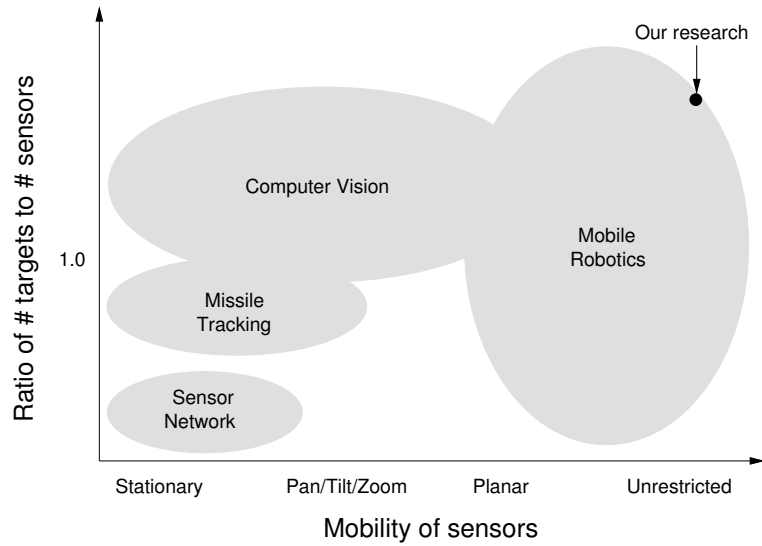


Figure 2.1: Research on the target tracking problem: Target tracking research performed by different communities can be categorized according to tracker mobility and the ratio of the number of trackers to the number of targets.

the thesis utilize multiple mobile robots to track moving objects, and assumes that the number of objects are bigger than the number of robots. Therefore, the work is projected on the top-left corner in Figure 2.1.

Chapter 3

Moving Object Tracker

As described in Section 1.1, the target tracking algorithm for an individual robot is decoupled from the cooperative tracking algorithm for a multi-robot system. This chapter describes our single-robot tracking algorithm as a basis layer of the cooperative multi-robot system. We make the following assumptions:

Target For most surveillance or security applications, motion is the most interesting feature to track. Therefore, we designed a single-robot tracker that tracks and reports the positions of *moving objects* in the vicinity of a robot.

Environment As explained in Chapter 1, mobile robots are required to have a motion estimation capability for safe navigation, especially in outdoor environments, which contain diverse movements. For this reason, a populated, unstructured *outdoor environment* is assumed.

Sensor The combination of a *camera* and a *laser rangefinder* is used for motion estimation in 3D space. Since a camera image contains rich information of object motion, a single camera is utilized for motion detection and tracking. A laser rangefinder provides depth information of image pixels for partial 3D position estimation.

3.1 Problem Statement Revisited

Section 1.1 describes the definition of the multiple target tracking problem using multiple mobile robots. In a similar way, the multiple target tracking problem using a single robot is defined here.

Input A single mobile robot and multiple moving targets in the vicinity of the robot

Output Positions and velocities of moving targets in the robot's local coordinate system

Goal To detect the moving targets and track their motions robustly

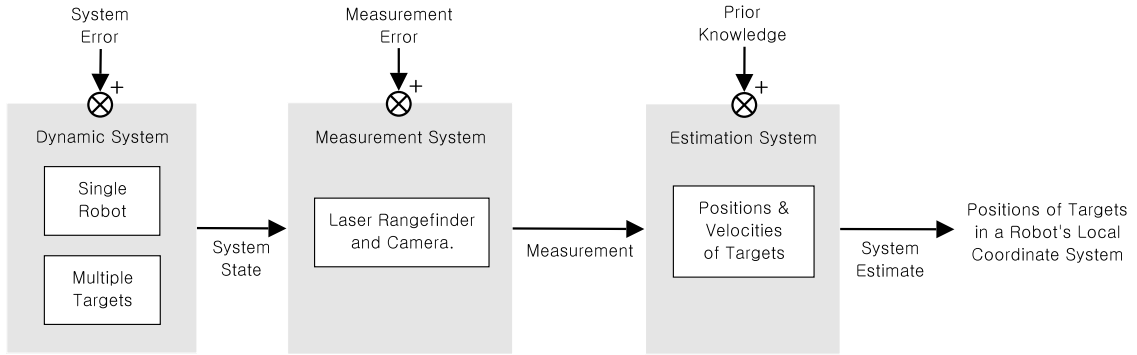


Figure 3.1: Multiple Target Tracking using a Single Robot: The problem is to estimate the positions of multiple targets in a robot's local coordinate system.

Restriction Real-time response and no prior knowledge on the number of targets or a target motion model

Figure 3.1 provides a pictorial description. The input system consists of a single robot and N targets, and the available measurements are images from a monocular camera and distance information from a laser rangefinder. The control of a robot is not involved in the estimation process since the motion commands for individual robots are generated by a high-level, cooperative behavior module described in Chapter 4. All computation must be done in real-time since the output of the algorithm will be fed into a robot control loop.

For moving object detection using a monocular camera, frame differencing, which compares two consecutive image frames and finds moving objects based on the difference, is the most intuitive and fast algorithm, especially when the viewing camera is static. However, when the camera moves (*eg.* when it is mounted on a mobile robot), straightforward differencing is not applicable because a big difference is generated by simply moving the camera even if nothing moves in the environment. There are two *independent motions* involved in the moving camera scenario: motions of moving objects and the ego-motion of the camera. Since these two motions are blended into a single image, the ego-motion of the camera needs to be eliminated so that the remaining motions, which are due to moving objects, can be detected. Figure 3.2 shows the processing sequence of our moving object tracking algorithm. Frame differencing is utilized, but the ego-motion of the camera in the previous image ($Image(t - 1)$) is compensated before comparing it with the current image ($Image(t)$). The detailed ego-motion compensation step is described in Section 3.3.

Real outdoor images are contaminated by various noise sources, *eg.* poor lighting conditions, camera distortion, unstructured and changing shape of objects, etc. Thus perfect ego-motion

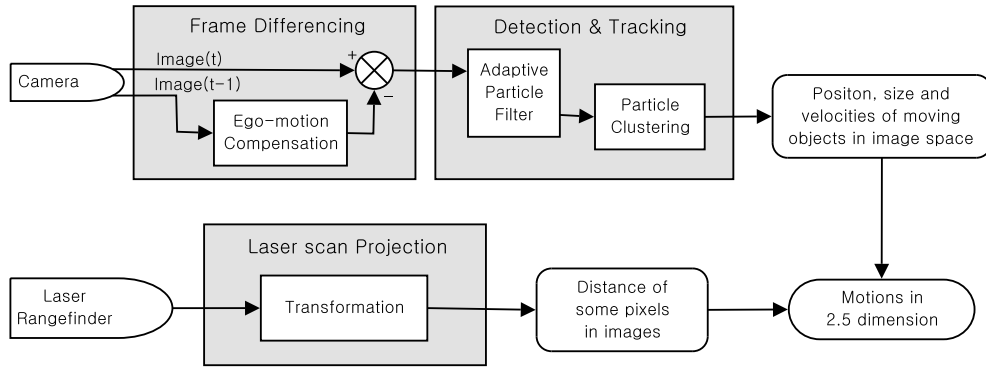


Figure 3.2: Processing sequence for moving object tracking from a mobile robot: The ego-motion of a robot should be eliminated so that remaining motions, which are caused by moving objects, can be detected. The laser scans provide the distance information of the moving objects.

compensation is rarely achievable. Even assuming that the ego-motion compensation is perfect, the difference image would still contain structured noise on the boundaries of objects because of the lack of depth information from a monocular image. Some of these noise terms are transient and some of them are constant over time. We use a probabilistic model to filter them out and to perform robust detection and tracking. The probability distribution of moving objects in image space is estimated using an adaptive particle filter (Fox, 2001). The particle filter design is discussed in Section 3.4.

Once the positions and velocities of moving objects are estimated in 2-dimensional image space, the information should be combined with the partial depth information from a laser rangefinder in order to construct full 3-dimensional motion models. By projecting range values into an image space, the image pixels at the same height as the laser rangefinder will have depth information. Section 3.5 provides more details.

3.2 Related Work

The computer vision community has proposed various methods to stabilize camera motions by tracking features (Censi et al., 1999; Tomasi and Kanade, 1991; Zoghلامي et al., 1997) and computing optical flow (Irani et al., 1994; Lucas and Kanade, 1981; Srinivasan and Chellappa, 1997). These approaches focus on how to estimate the transformation (*homography*) between two image coordinate systems. However, the motions of moving objects are typically not considered, which leads to poor estimation.

Other approaches that extend these methods for motion tracking using a pan/tilt camera include those in (Foresti and Micheloni, 2003; Murray and Basu, 1994; Nordlund and Uhlin, 1996).

However, in these cases the camera motion was limited to translation or rotation. When a camera is mounted on a mobile robot, the main motion of the camera is a forward/backward movement, which makes the problem different from that of a pan/tilt camera.

There is other research on tracking from a mobile platform with similar motions. Yilmaz et al. (2001) track a single object in forward-looking infrared (FLIR) imagery taken from an airborne, moving platform, and Behrad et al. (2001), van Leeuwen and Groen (2002) track cars in front using a camera mounted on a vehicle driven on a paved road.

Once motion has been identified, objects in the scene need to be tracked. Work focusing on robust multiple target tracking using probabilistic filters includes (Schultz et al., 2001) which uses a particle filter to track people indoors (corridors) using a laser rangefinder, and (Hue et al., 2001) which also uses a particle filter to track multiple objects using a stationary camera. A Kalman filter was used in (Kang et al., 2002) to detect and track human activity with the combination of a static camera and a moving camera.

3.3 Ego-motion Compensation

The ego-motion of the camera can be estimated by tracking features between images (Censi et al., 1999; Foresti and Micheloni, 2003; Zoghلامي et al., 1997). When the camera moves, two consecutive images, I^t (the image at time t) and I^{t-1} (the image at time $t - 1$), are in different coordinate systems. Ego-motion compensation is a transformation from the image coordinates of I^{t-1} to that of I^t so that the two images can be compared directly. The transformation can be estimated using two corresponding feature sets: a set of features in I^t and a set of corresponding features in I^{t-1} . However, since there are independently moving objects in the images, a transform model and outlier detection algorithm needs to be designed so that the result of ego-motion compensation is not sensitive to object motions.

3.3.1 Feature Selection and Tracking

We adopt the feature selection algorithm introduced in (Tomasi and Kanade, 1991) for corresponding feature set selection. Given a single image frame, a small search window runs over the whole image to check if the window contains a “*reliably trackable*” feature. For each search window,

1. Compute the boundary information, $\left[\frac{\partial I(x,y)}{\partial x} \quad \frac{\partial I(x,y)}{\partial y} \right]^T$
2. Compute the covariance matrix of the boundary pixels

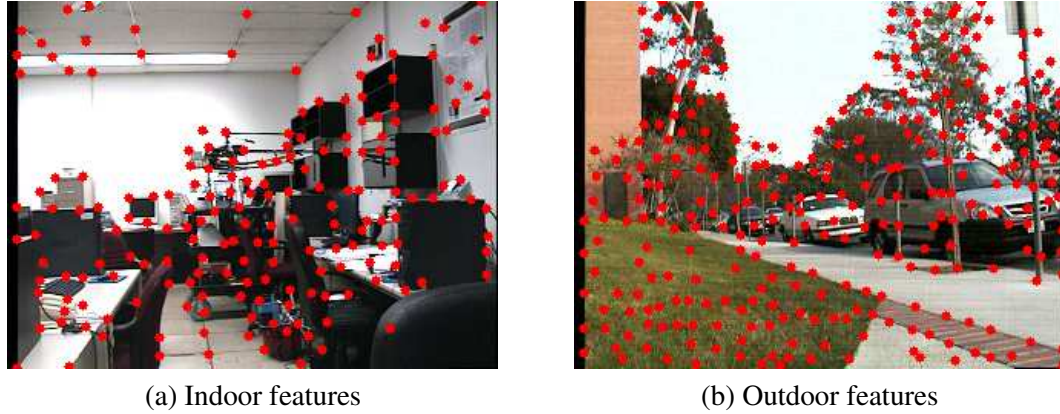


Figure 3.3: Saliient features selected for tracking: Primarily perpendicular patterns (*eg.* corners) or divergent textures (*eg.* leaves) are selected.

3. Compute two eigenvalues (λ_1, λ_2) of the covariance matrix
4. Select a search window such that $\min(\lambda_1, \lambda_2) > \theta$

Search windows with two small eigenvalues contain no pattern, and those with one small eigenvalue and one big eigenvalue contain unidirectional patterns, which are not easy to track. Only search windows with two big eigenvalues are selected for tracking because they contain a perpendicular pattern (*eg.* corners) or divergent textures (*eg.* leaves) which are relatively unique enough to be tracked. Figure 3.3 shows the features (filled circles) selected from indoor and outdoor images. In the indoor image, most of the selected features are the corners of objects, like desks, computers, and bookshelves. In the outdoor image, some corners of bricks and cars, and leaves and grass that have complex textures were selected as features.

The feature selection algorithm runs on images (I^{t-1}), and generates features (f^{t-1}). The *Lucas-Kanade* method (Forsyth and Ponce, 2003; Lucas and Kanade, 1981) is applied to track those features on the subsequent image (I^t) to find the corresponding set of features (f^t). For efficiency, the search range was limited to a small constant distance (assuming a bounded robot speed). The pyramid technique (Bouguet, 1999) is used for fast computation. Figure 3.4 shows the robustness of the tracking method. Figure 3.4 (a) shows the features selected from the image I^t , and Figure 3.4 (b) shows the same features tracked over 30 frames on the image I^{t+30} , which is an image captured 3 seconds later. The erroneous features on image boundaries are eliminated for subsequent processing.

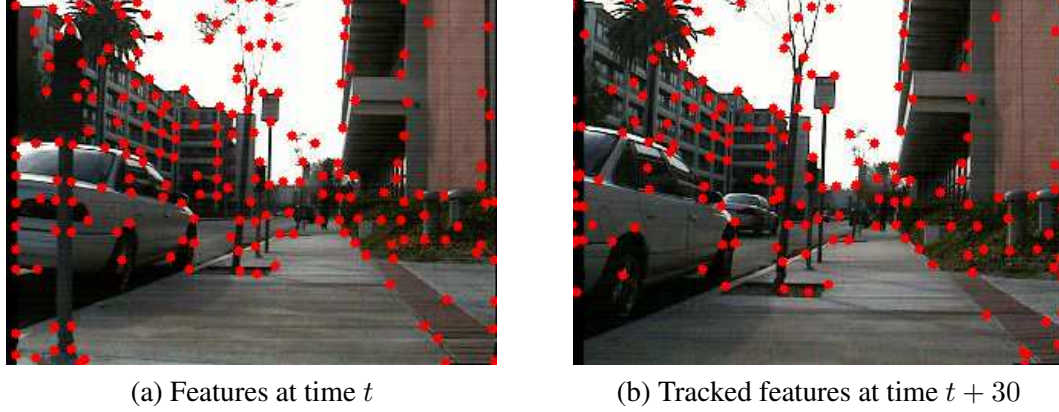


Figure 3.4: Feature tracking: (a) shows salient features selected, and (b) shows the same features tracked over 30 frames (3 seconds).

3.3.2 Transformation Estimation

Once the correspondence $\langle f^{t-1}, f^t \rangle$ is known, the ego-motion of the camera can be estimated using a transformation model and an optimization method. We have studied three different models: affine model, bilinear model, and pseudo-perspective model.

$$\begin{aligned}
 \text{Affine : } & \begin{bmatrix} f_x^t \\ f_y^t \end{bmatrix} = \begin{bmatrix} a_0 f_x^{t-1} + a_1 f_y^{t-1} + a_2 \\ a_3 f_x^{t-1} + a_4 f_y^{t-1} + a_5 \end{bmatrix} \\
 \text{Bilinear : } & \begin{bmatrix} f_x^t \\ f_y^t \end{bmatrix} = \begin{bmatrix} a_0 f_x^{t-1} + a_1 f_y^{t-1} + a_2 + a_3 f_x^{t-1} f_y^{t-1} \\ a_4 f_x^{t-1} + a_5 f_y^{t-1} + a_6 + a_7 f_x^{t-1} f_y^{t-1} \end{bmatrix} \\
 \text{Pseudo-perspective : } & \begin{bmatrix} f_x^t \\ f_y^t \end{bmatrix} = \begin{bmatrix} a_0 f_x^{t-1} + a_1 f_y^{t-1} + a_2 + a_3 f_x^{t-1 2} + a_4 f_x^{t-1} f_y^{t-1} \\ a_5 f_x^{t-1} + a_6 f_y^{t-1} + a_7 + a_4 f_x^{t-1} f_y^{t-1} + a_3 f_y^{t-1 2} \end{bmatrix}
 \end{aligned} \tag{3.1}$$

When the interval between consecutive images is very small, most ego-motions of the camera can be estimated using an affine model, which can cover translation, rotation, shearing, and scaling motions. However, when the interval is long¹, the camera motion in the interval cannot be captured by a simple linear model. For example, when the robot moves forward, the features in the image center move slower than those near the image boundary, which is a projection, not a zoom. Therefore, a nonlinear transformation model is required for our case. On the other hand, an over-fitting problem may be caused when a model is highly nonlinear, especially when some of the selected features are associated with moving objects (*outliers*). There is clearly a trade-off

¹We obtain camera data at 5 Hz



Figure 3.5: Outlier feature detection: Outliers are marked in red, filled circles, and inliers are marked in green, empty circles.

between a simple, linear model and a highly nonlinear model, and it needs more empirical research for the best selection. We used a bilinear model for the experiments reported in this thesis proposal.

Given a transformation model (T_t), the cost function for least square optimization is defined as:

$$J = \frac{1}{2} \sum_{i=1}^N (f_i^t - T_{t-1}^t (f_i^{t-1}))^2 \quad (3.2)$$

where N is the number of features. The model parameters for ego-motion compensation are estimated by minimizing the cost. However, as mentioned before, some of the features are associated with moving objects, which lead to the inference of an inaccurate transformation. Those features (outliers) should be eliminated from the feature set before the final transformation is computed. The model parameter estimation is thus performed using the following two-step procedure:

1. compute the initial estimate T_0 using the full feature set F .
2. partition the feature set F into two subsets F_{in} and F_{out} as:

$$\begin{cases} f_i \in F_{in} & \text{if } |f_i^t - T_{0,t-1}^t (f_i^{t-1})| < \epsilon \\ f_i \in F_{out} & \text{otherwise} \end{cases} \quad (3.3)$$

3. re-compute the final estimate T using the subset F_{in} only.

Figure 3.5 shows the partitioned feature sets: F_{in} is marked with empty circles, and F_{out} is marked with filled circles. Note that all features associated with the pedestrian are detected as

outliers. It is assumed for outlier detection that the portion of moving objects in the images is relatively smaller compared to the background; the features which do not agree with the main motion are considered as outliers. This assumption will break when the moving objects are very close to the camera. However, most of the time, these objects pass by the camera in a short period (leading to transient errors), and a high-level probabilistic filter is able to deal with the errors without total failure.

3.3.3 Frame Differencing

Image I^{t-1} is converted using the transformation model before being compared to the image I^t in order to eliminate the effect of the camera ego-motion. For each pixel (x, y) :

$$I_{comp}(x, y) = I_{t-1} \left(T_{t-1}^t{}^{-1}(x, y) \right) \quad (3.4)$$

Figure 3.6 (c) shows the compensated image of Figure 3.6 (a); the translational and forward motions of the camera were clearly eliminated. The valid region \mathfrak{R} of the transformed image is smaller than that of the original image because some pixel values on the border are not available in the original image I^{t-1} . The invalid region in Figure 3.6 (c) is filled black. The difference image between two consecutive images is computed using the compensated image:

$$I_{diff}(x, y) = \begin{cases} |(I_{comp}(x, y) - I_t(x, y))| & \text{if } (x, y) \in \mathfrak{R} \\ 0 & \text{otherwise} \end{cases} \quad (3.5)$$

Figure 3.7 compares the results of two cases: frame differencing without ego-motion compensation (Figure 3.7 (a)) and with ego-motion compensation (Figure 3.7 (b)). The results show that the ego-motion of a camera is decomposed and eliminated from image sequences.

3.4 Motion Detection in 2D Image Space

The *Frame Differencing* step in Figure 3.2 generates the difference images, $I_{diff}^0, I_{diff}^1, \dots, I_{diff}^t$, whose normalized pixel values represent the probability of moving objects. Based on the sequence of these difference images, the position and size of the moving objects are estimated. This estimation process can be written using a Bayesian formulation. Let \mathbf{x}^t represent the position of a moving object and $P_m(\mathbf{x}^t)$ be the posterior probability distribution of the object:



(a) Image at time $t - 1$



(b) Image at time t



(c) Compensated image of (a)

Figure 3.6: Image Transformation: (c) is the transformed image of (a) into (b) coordinates. The valid region of the compensated image is smaller than that of the original image due to the absence of data on the border.



(a) Difference without compensation



(b) Difference with compensation

Figure 3.7: Results of frame differencing: (b) shows that the ego-motion of a camera was decomposed and eliminated from image sequences.

$$\begin{aligned}
P_m(\mathbf{x}^t) &= P(\mathbf{x}^t | I_{diff}^0, I_{diff}^1, \dots, I_{diff}^t) \\
&= \alpha^t P(I_{diff}^t | \mathbf{x}^t, I_{diff}^0 \dots, I_{diff}^{t-1}) P(\mathbf{x}^t | I_{diff}^0 \dots, I_{diff}^{t-1}) \\
&= \alpha^t P(I_{diff}^t | \mathbf{x}^t) P(\mathbf{x}^t | I_{diff}^0 \dots, I_{diff}^{t-1}) \\
&= \alpha^t P(I_{diff}^t | \mathbf{x}^t) \int P(\mathbf{x}^t | I_{diff}^0 \dots, I_{diff}^{t-1}, \mathbf{x}^{t-1}) P(\mathbf{x}^{t-1} | I_{diff}^0 \dots, I_{diff}^{t-2}) d\mathbf{x}^{t-1} \\
&= \alpha^t P(I_{diff}^t | \mathbf{x}^t) \int P(\mathbf{x}^t | \mathbf{x}^{t-1}) P(\mathbf{x}^{t-1} | I_{diff}^0 \dots, I_{diff}^{t-2}) d\mathbf{x}^{t-1} \\
&= \alpha^t P(I_{diff}^t | \mathbf{x}^t) \int P(\mathbf{x}^t | \mathbf{x}^{t-1}) P_m(\mathbf{x}^{t-1}) d\mathbf{x}^{t-1}
\end{aligned} \tag{3.6}$$

3.4.1 Particle Filter Design

The *Particle filter* (Isard and Blake, 1998; Thrun et al., 2001) is a simple but effective algorithm to estimate the posterior probability distribution recursively, which is appropriate for real-time applications. In addition, its ability to perform multi-modal tracking is attractive for multiple object detection and tracking. An efficient variant, called the *Adaptive Particle Filter*, was introduced in (Fox, 2001). This changes the number of particles dynamically for a more efficient implementation. We implemented the *Adaptive Particle Filter* to estimate the posterior probability distribution in Equation 3.6.

Particle filters require two models for the estimation process: an action model and a sensor model. A constant-velocity action model was assumed for moving object detection. Where an i_{th} particle is defined as $s^t = [x \ y]^T$ and Δt is a time interval,

$$s_i^{t+1} = s_i^t + \Delta t \times \dot{s}_i^t + Normal\left(\frac{\gamma}{\omega_i^t}\right) \tag{3.7}$$

Parameterized noise is added to the constant-velocity model in order to overcome an intrinsic limitation of the particle filter, which is that all particles move in a converging direction. However, a dynamic mixture of divergence and convergence is required to detect newly introduced moving objects. (Thrun et al., 2001) introduced a mixture model to solve this problem, but in the image space the probability $P(\mathbf{x}^t | I_{diff}^t)$ is uniform and the dual MCL becomes random. Therefore, we used a simpler, but effective method by adding inverse-proportional noise. For the sensor model, the normalized difference image (I_{diff}) is directly used as sensor input. The particle filter uses a $m \times m$ fixed-size mask (usually 5×5) to evaluate each particle. By using the mask, salt-and-pepper noise can be eliminated.

Table 3.1: Adaptive Particle Filter Algorithm

Initialization:

generate a random sample set S with the size N_{max}
 set the importance factor ω of each particle s uniformly
 $n = N_{max}$

Update:

$S' = \phi$
 $n' = 0$
 do
 draw random s from S according to $\omega_1, \dots, \omega_n$
 $\omega = \frac{1}{m^2} \sum_{j=-m/2}^{m/2} \sum_{k=-m/2}^{m/2} I_{diff}(s(x) - j, s(y) - k)$
 $s' = s + \Delta t \times \dot{s} + Normal(\frac{\sigma}{\omega})$
 $\omega' = \frac{1}{m^2} \sum_{j=-m/2}^{m/2} \sum_{k=-m/2}^{m/2} I_{diff}(s'(x) - j, s'(y) - k)$
 add $\langle s', \omega' \rangle$ to S'
 $n' = n' + 1$
 until $n' < N_{min}$ or $n' < \frac{1}{2\epsilon} \chi_{k-1, 1-\delta}^2$
 normalize ω in S'
 return $\langle S', n' \rangle$

$$\omega_i^t = \frac{1}{m^2} \sum_{j=-m/2}^{m/2} \sum_{k=-m/2}^{m/2} I_{diff}(s_i^t(x) - j, s_i^t(y) - k) \quad (3.8)$$

The final algorithm of the particle filter is described in Table 3.1.

Figure 3.8 (b) shows the output of the particle filter. The dots represent the position of particles, and the horizontal bar on the top-left corner of the image shows the number of particles being used.

3.4.2 Particle Clustering

The particle filter generates a set of weighted particles that estimate the posterior probability distribution of moving objects, but the particles are not easy to process in the following step. More intuitive and meaningful data can be extracted by clustering the particles. Given the estimated posterior distribution using particles, a mixture of Gaussians is inferred corresponding to the

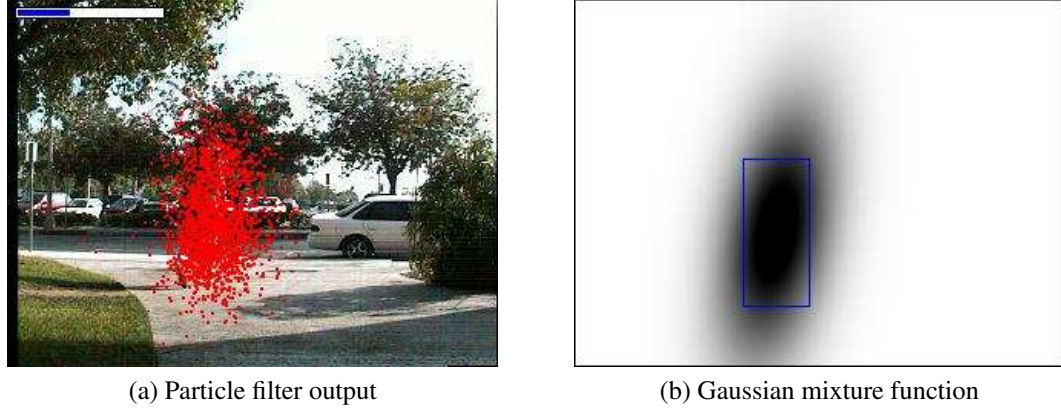


Figure 3.8: Particle filter tracking: Red dots in the image (a) represent the position of particles, and the horizontal bar on the top-left corner of the image (a) shows the number of particles being used. (b) shows the Gaussian mixture function and the extracted region of the pedestrian.

posterior distribution using the *Expectation-Maximization* (EM) algorithm (Hastie et al., 2001). The Gaussian mixture function represents the original posterior distribution and the regions of moving objects can be extracted by thresholding the Gaussian mixture function. Figure 3.8 (c) shows the Gaussian mixture function, and the blue rectangle indicates the extracted region of the pedestrian in the input image. For real-time response, the maximum iterations of the EM algorithm is fixed to a constant.

3.5 Position Estimation in 3D Space

A monocular image provides rich information for ego-motion compensation and motion tracking in 2-dimensional image space. However, a single camera has limit on retrieving depth information, and an additional sensor is required to construct full 3-dimensional models of moving objects. Our robots are equipped with a laser rangefinder, which provides depth information within a single plane. Given the optical properties of a camera and the transformation between the camera and the laser rangefinder, distance information from the laser rangefinder can be projected onto the image coordinates (Figure 3.9).

Given the heading α and the range r of a scan, the projected position (x, y) in the image coordinate system is computed as follows:

$$\begin{bmatrix} x \\ y \end{bmatrix} = \begin{bmatrix} \frac{w}{2} \times \left(1 - \frac{\tan(\alpha)}{\tan(f_h)}\right) \\ \frac{h}{2} \times \left(1 + \left(d - \frac{d}{r} \times (r - l)\right) \times \frac{1}{l \times \tan(f_v)}\right) \end{bmatrix} \quad (3.9)$$

Table 3.2: Expectation-Maximization Algorithm for Particle Clustering

Initialization:

set each mean μ_i randomly following uniform distribution
 set each covariance matrix Σ_i identity matrix
 set the weight π_i of each Gaussian uniformly

Expectation Step:

for each Gaussian m and particle s_i ,

$$z_m^i = \frac{P(s_i|\mu_m, \Sigma_m) \pi_m}{\sum_{k=1}^{M_{max}} P(s_i|\mu_k, \Sigma_k) \pi_k} \quad \text{where } P(s|\mu, \Sigma) \text{ is bi-variate Gaussian}$$

Maximization Step:

for each Gaussian m ,

$$\mu_m = \frac{\sum_{i=1}^{N_{max}} z_m^i (s_i - \mu_m)(s_i - \mu_m)^T}{\sum_{i=1}^{N_{max}} z_m^i}$$

$$\Sigma_m = \frac{\sum_{i=1}^{N_{max}} z_m^i s_i}{\sum_{i=1}^{N_{max}} z_m^i}$$

$$\pi_m = \frac{\sum_{i=1}^{N_{max}} z_m^i}{N_{max}}$$

Estimation:

repeat *Expectation Step* and *Maximization Step* until it converges
 or reaches the maximum iteration
 return only Gaussians with $\pi_m > \xi$

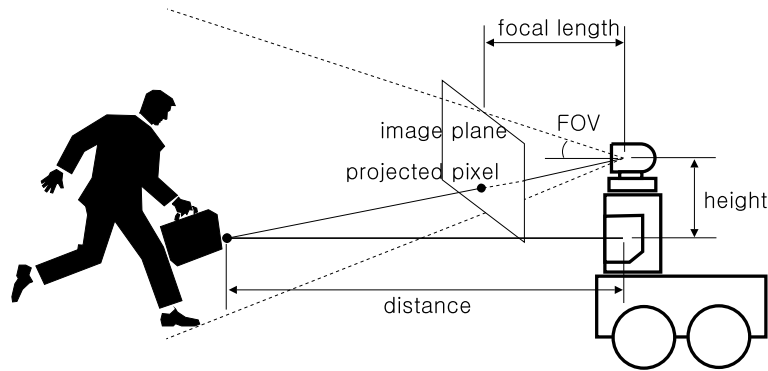


Figure 3.9: Projection of laser scans onto the image coordinates: The range scans from a laser rangefinder can be projected onto the image coordinate system based on the optical properties of a camera and the transformation between the camera and the laser rangefinder.



Figure 3.10: Projected laser scans: The image pixels at the same height as the laser rangefinder have depth information.

where the focal length of the camera is l , the horizontal and vertical field-of-view of the camera are f_h and f_v , the height from the laser rangefinder to the camera is d , and the image size is $w \times h$. This projection model assumes a very simple camera model (a pin-hole camera) for fast computation. As a result of the projection, the image pixels at the same height as the laser rangefinder will have depth information as shown in Figure 3.10. For ground robots, this partial 3D information can be enough for safe navigation assuming all moving obstacles are on the the same plane as the robot. In terms of moving object tracking, if the region of a moving objects in an image space and those pixels are overlapped, then the distance between a robot and the moving object can be estimated. The position in the partial 3D space $[x \ y \ h]^T$ is returned as the final estimation result.

Initial test for the integration of the 2D motion estimates and range scans from a laser rangefinder was promising. However, more work is required for robust estimation, *eg.* additional filter design to overcome the asynchronous sensor inputs. This future work will be discussed in Section 3.7.

3.6 Experiments

3.6.1 Experimental Setup

The algorithms were implemented and tested in various outdoor environments using three different robot platforms: robotic helicopter, Segway RMP, and Pioneer2 AT. Each platform has unique characteristics in terms of its ego-motion. The *Robotic Helicopter* (Saripalli et al., 2003) in Figure 3.11 (a) is an autonomous flying vehicle carrying a monocular camera facing downward. Once it takes off and hovers, planar movements are the main motion, and moving objects on the ground stay at a roughly constant distance from the camera most of the time; however,

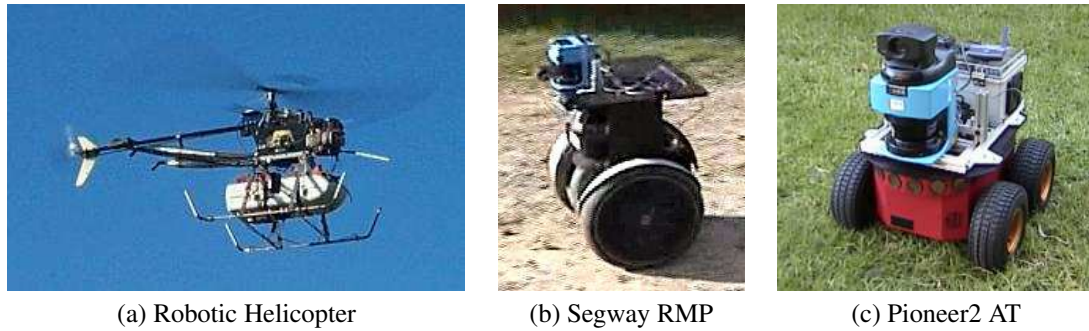


Figure 3.11: Robot platforms for experiments: Each platform has unique characteristics in terms of its ego-motion.

pitch and roll motions for a change of direction still generate complicated video sequences. Also, high-frequency vibration of the engine adds motion-blur to camera images.

The *Segway RMP* in Figure 3.11 (b) is a two-wheeled, dynamically stable robot with self-balancing capability. It works like an inverted pendulum; the wheels are driven in the direction that the upper part of the robot is falling, which means the robot body pitches whenever it moves. Especially when the robot accelerates/decelerates, the pitch angle increases by a significant amount. Since all sensors are directly mounted on the platform, the pitch motions prevent direct image processing. Therefore, the ego-motion compensation step should be able to cope with not only planar movements but also pitch motions.

The *Pioneer2 AT* in Figure 3.11 (c) is a typical four-wheeled, statically stable robot. Since the *Pioneer2* robot is the only statically stable platform among these robot platforms, we drove the robot on the most severe test environment. Figure 3.14 and Figure 3.17 show the rocky terrain where the robot was driven. In addition, the moving objects were occluded occasionally because of the trees in the environment.

The computation was performed on embedded computers (Pentium III 1GHz) on the robots. Low resolution (320x240 pixels) input images were chosen for real-time response, and the tracking algorithm was able to process five frames per second. Since the algorithm is supposed to run in parallel with other processes (eg. navigation and communication), less than 70 percent of the CPU time was dedicated for tracking.

3.6.2 Experimental Results

The snapshots of the particle filter tracking moving objects are shown in Figure 3.12–3.14. The maximum number of particles was set to 5,000, and the minimum number of particles was set

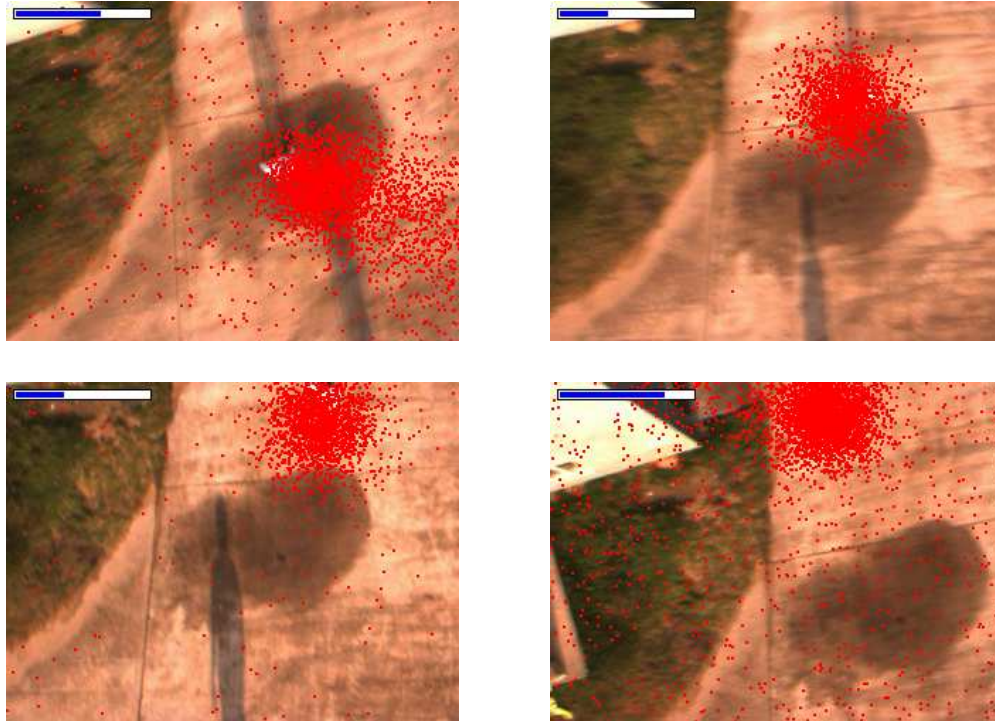


Figure 3.12: Snapshots of particle filter tracking a moving object: from Robotic helicopter

to 500. The figures show that the particle filter reduces the number of particles for efficient estimation when it converges.

The performance of the tracking algorithm was evaluated by comparing to the positions of manually tracked objects. For each video sequence, the rectangular region of moving objects were marked manually and used as ground truth. Figure 3.15–3.17 shows this evaluation process. The left windows show the input images, and the right windows show the posterior distribution (Gaussian mixture) functions. The thick rectangles indicate the position of manually-tracked objects, the thin rectangles indicate the output of the tracking algorithm, and the thin lines show the distance between the center of the rectangles. The final evaluation result is shown in Table 3.3. *Motions* is the number of moving objects over the total number of frames. *Detected* is the total number of detected objects, and *True +* and *False +* are the number of correct detections and the number of false-positives. *Detection Rate* shows the percentage of moving objects correctly detected, and *Avg. Error* is the average Euclidean distance in pixels between the ground truth and the output of tracking algorithm. The average distance error should not be considered as actual error measurement since the tracking algorithm does not perform an explicit object segmentation; it may track a part of an object that generates motion while the ground truth always tracks the whole objects even though only part of the object moves.

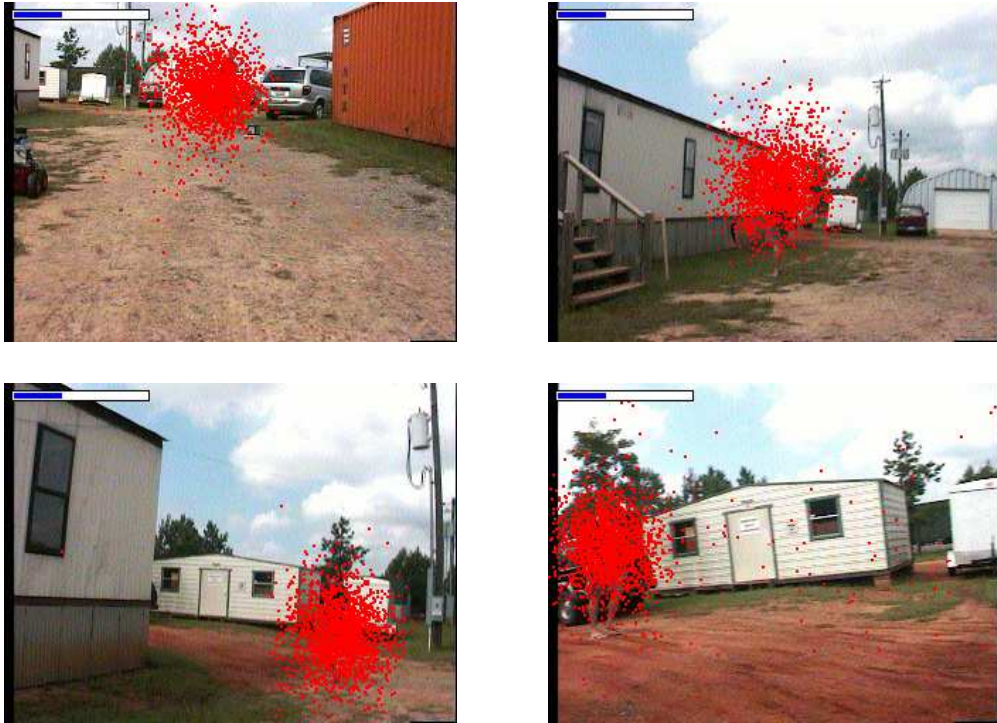


Figure 3.13: Snapshots of particle filter tracking a moving object: from Segway RMP



Figure 3.14: Snapshots of particle filter tracking a moving object: from Pioneer2 AT

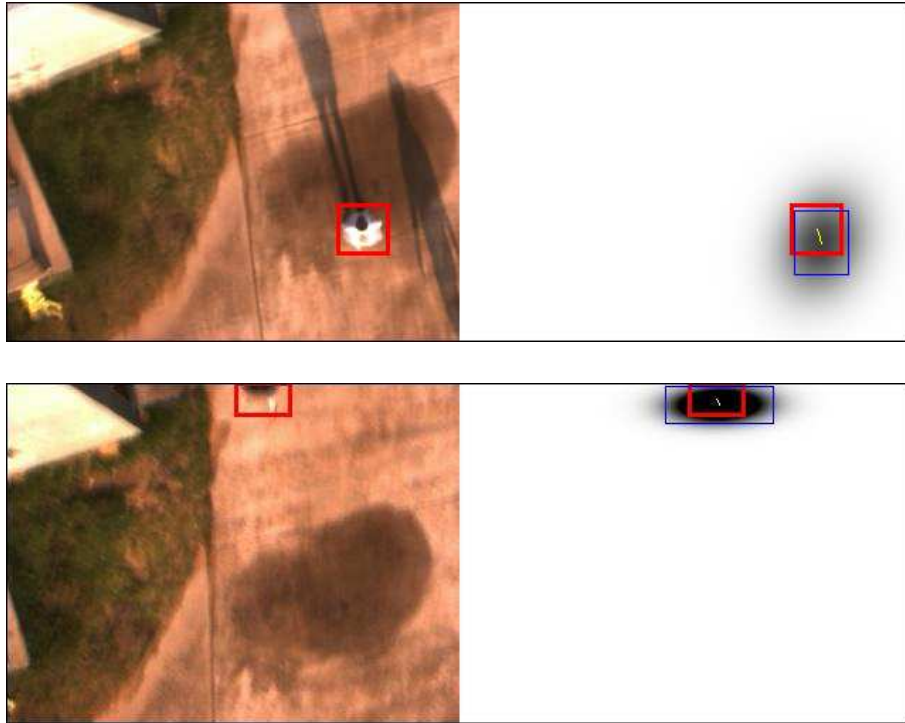


Figure 3.15: Performance evaluation: tracking from Robotic helicopter

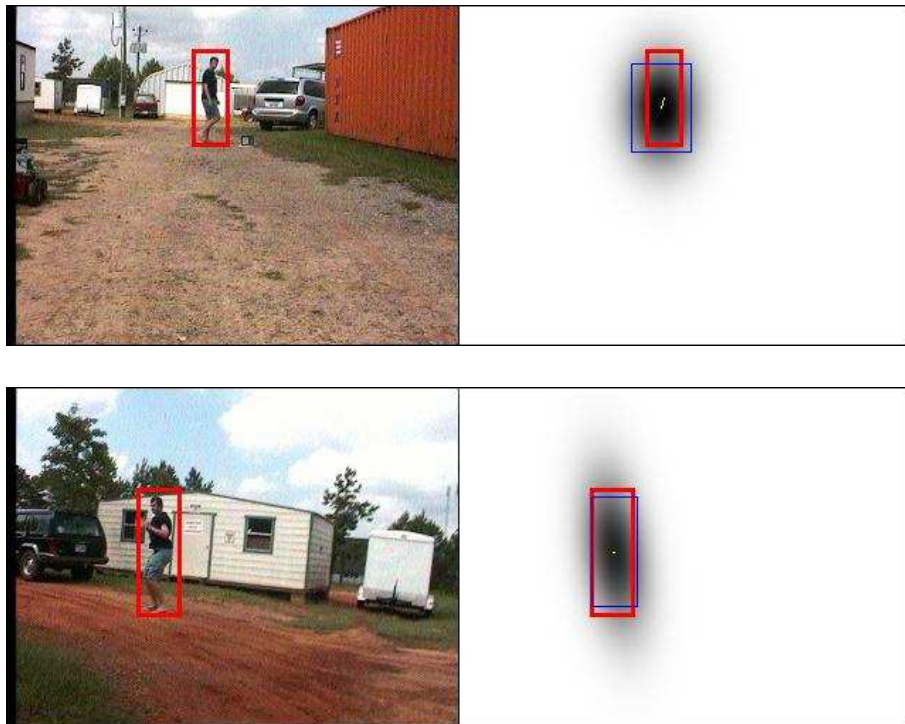


Figure 3.16: Performance evaluation: tracking from Segway RMP

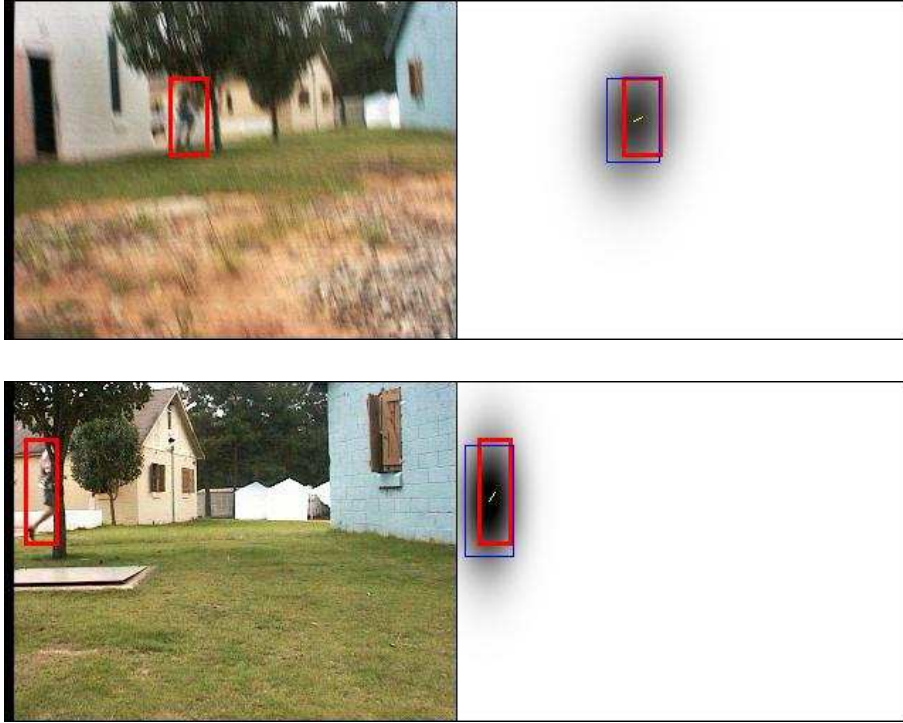


Figure 3.17: Performance evaluation: tracking from Pioneer2 AT

Platform	Motions	Detected	True +	False +	Detection Rate	Avg. Error
Robotic helicopter	35 / 43	29	29	0	82.86 %	13.26
Segway RMP	220 / 230	208	206	2	93.63 %	20.29
Pioneer2 AT	172 / 195	126	114	12	66.28 %	13.54

Table 3.3: Performance of moving object detection algorithm

The *Robotic helicopter* result shows that the tracking algorithm missed six objects, but five of them were the cases when a moving object was introduced and showed only partially on the boundary of the image plane. Once the whole object entered into the camera field-of-view, the tracking algorithm detected it robustly. For the *Segway RMP* result, the detection rate was satisfactory, but the average distance error was larger than the others. The reason was that the walking person was closer to the robot and the tracking algorithm often detected the upper body only, which caused a constant distance error. The *Pioneer2 AT* result was the worst; however, as explained in the previous section, the terrain for the experiment was more challenging and the input images were more blurred and unstable.

3.7 Discussion

The individual motion tracker using a camera showed stable motion-tracking capability in 2D image space by adopting a probabilistic filter at the end of the processing sequence. However, the tracker sometimes generates transient position errors in 3D space when the rotational velocity of the robot is high. The conversion from 2D to 3D using a laser rangefinder assumes perfect synchronization between a camera and a laser rangefinder, which is unachievable in real-robot experiments. Since there is always unknown delay between the image capture time and the range retrieval time, laser range scans are projected at wrong places when a robot rotates at high speed. We believe that such errors can be reduced by adding a second probabilistic filter for 3D-position estimation, or by modifying the current probabilistic filter such that the measurement model includes not only difference images but also projected distance information. This is part of our future research plan.

Chapter 4

Cooperative Multi-Target Tracking

A cooperative motion strategy for multiple target tracking system is presented in this chapter. The single-robot tracking algorithm was described in Chapter 3; this capability is subsumed within the multi-robot system design.

4.1 Problem Statement Revisited

When the sensors of a tracking system are mobile robots, tracking performance can be improved by re-positioning robots in response to the motion changes of targets. As explained in Section 2.1.6, there are two kinds of cooperations: *uncertainty reduction* and *task allocation*. The latter type of cooperation is considered in this thesis. The precise problem statement is:

Input Estimated poses of M robots and estimated positions of n tracked targets (out of total N targets) in a bounded environment ($M \ll N$)

Output Motion commands for M robots

Goal Maximize the number of tracked targets n over time T

$$Observation = \sum_{t=0}^T \frac{n}{N} \times \frac{1}{T} \times 100 \quad (4.1)$$

Constraints No prior knowledge of the number of robots or targets, and no target motion model.

The multi-target tracking problem using a group of mobile robots can be treated as a task allocation problem; given a group of agents (*robots*) and a group of tasks (*targets*), assign each task to the proper agent so that the overall performance (*the total number of tracked targets over time*) is maximized. However, when the number of targets N is much bigger than the number of

robots M , it is not preferable to compute the allocation of individual targets because of increasing complexity of allocation algorithm. We propose a *Region-based Approach* as a more efficient target allocation method; targets are grouped by the current positions, and each robot is allocated to a group of targets.

The *Region-based Approach* algorithm is described conceptually in Section 4.3. In the following sections, the algorithm is specialized for restricted real-world environments. Section 4.4 explains how the algorithm can be implemented on a real system for unstructured environments, and Section 4.5 suggests a coarse discretization of the algorithm for structured environments by exploiting environmental features.

4.2 Related Work

Various distributed algorithms have been proposed for multi-robot coordination with applications to multi-target tracking. The ALLIANCE architecture (Parker, 1999) achieves target-assignment by the interaction of motivational behaviors. If a target was not tracked for a while, the robot which was supposed to track the target would give up and another robot in a better position would take up the target. In the BLE architecture (Werger and Matarić, 2000), if a particular robot thinks it is best suited to track a specified target, it stops other robots from tracking the target by broadcasting inhibition signals over the network. The Murdoch architecture (Gerkey and Matarić, 2001) showed that target-assignment problem can be solved using a principled publish/subscribe messaging model; the best capable robot is assigned to each tracking task using a one-round auction.

There have been other approaches that determine robot poses without explicit target assignment, especially when the ratio of the number of robots to the number of targets is close to 1.0. In (Spletzer and Taylor, 2003), the configuration of a team of mobile robots was actively controlled by minimizing the expected error in tracking target positions, and a reactive motion planner was reported in (Murrieta-Cid et al., 2002) that maximizes the shortest distance that a target needs to move in order to escape an observer's visibility region.

The Pursuit-Evasion problem introduced in (Yamashita et al., 1997) is a formally simplified tracking problem. The goal is to find continuously-moving intruders using a single or multiple searchers with flashlights that emit a single ray of light. Yamashita et al. (1997) presents upper and lower bounds of the number of necessary searchers in a given environment (a simple polygon) and four measures of shape complexity of the environment (the number of edges, the number of reflex vertices, the bushiness, and the size of a minimum guard set). Guibas et al. (1997) extend

the problem to exploit a visible area instead of a single ray of light. Several bounds on the number of pursuers are defined and the complete algorithm for a single pursuer case is presented.

4.3 Region-based Approach

The *Region-based Approach* is based on the following fundamental assumption:

For two comparably sized regions, more robots should be deployed in the one with the higher number of targets.

Instead of allocating targets to each robot, the mobile robots are allocated to each region based on the target distribution and robot distribution. The *robot density* and the *target density* are defined for each position in an environment, and a mobile robot is attracted to (or repulsed from) the position based on those density estimates. For example, the less targets a region has, the less robots the region requires, and the more robots the current region has, the more robots in that region are free to move to other regions. Our approach assumes the following:

Global Communication The robot poses and estimated target positions are exchanged among robots so that all robots can make decisions based on global information. However, the decision making is still distributed based on the collected information, which is maintained *independently*; the collected information can (and does in reality) vary from robot to robot.

Global Localization All robots share a global coordinate system so that the positions of targets detected by different robots can be translated into a single coordinates. Actual implementation of localization methods are explained in Chapter 5 and Chapter 6

Bounded Environment The size of an environment is bounded by the communication range among robots, not by the intrinsic limitation of our algorithm.

Robust Tracker The cooperative tracking algorithm is decoupled from the low-level target tracker; such a single-robot tracker is described in Chapter 3.

Unknown Target Model The cooperative tracking algorithm requires no prior knowledge of target maneuvers.

In order to demonstrate how a robot maintain the “*density estimates*” or determine the most “*urgent*” region in the following sections, we use the situation in Figure 4.1 as an example.

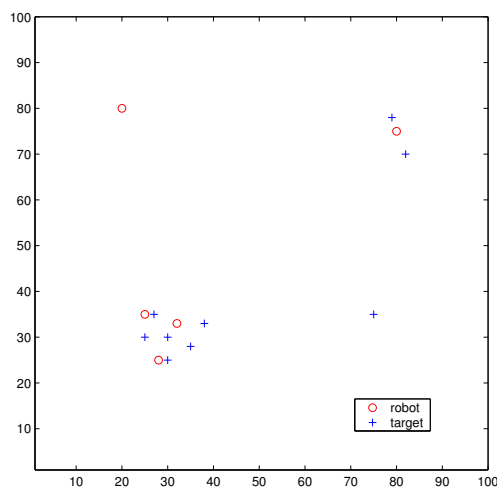


Figure 4.1: Positions of mobile robots and targets in a bounded environment: Red circles indicate the position of robots, and the blue crosses indicate the position of tracked targets.

4.3.1 Relative Density Estimates as Attributes of Space

In order to compute robot and target density values at each position, models for robot position, target position, and region boundary are required. Based on the output of a robot localization algorithm, the position of a robot can be modeled by a delta function or a Gaussian function. When the localization algorithm returns an exact position (\mathbf{x}_i) as the best estimate, the robot position is modeled using a delta function.

$$r_i = \delta(\mathbf{x}_i) \quad (4.2)$$

When the localization algorithm returns a center position (μ_i) as the best estimate and a covariance matrix (Σ_i) as uncertainty estimate, a bi-variate Gaussian model is adequate.

$$r_i = N(\mu_i, \Sigma_i) \quad (4.3)$$

The robot distribution r over an environment is computed by summing the individual models.

$$r = \sum_i \delta(\mathbf{x}_i) \quad (4.4)$$

$$r = \sum_i N(\mu_i, \Sigma_i) \quad (4.5)$$

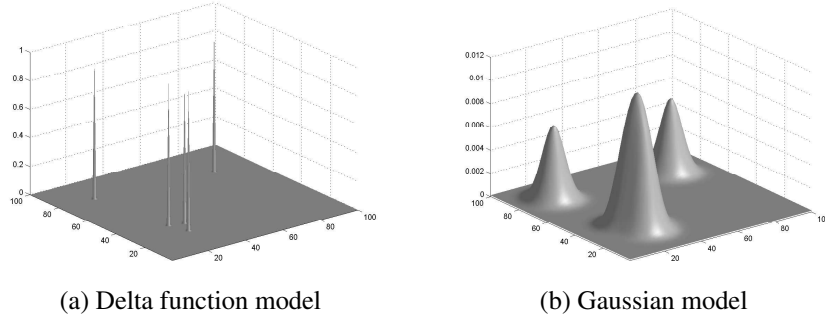


Figure 4.2: Robot distribution model: (a) is preferable when a robot localization method returns a position estimate only, and (b) is adequate when it returns both a position estimate and a uncertainty estimate. The positions of robots are shown in Figure 4.1.

Figure 4.2 (a) shows the robot distribution using the delta function model, and Figure 4.2 (b) shows the robot distribution using the bi-variate Gaussian model when the positions of robots are as in Figure 4.1.

In similar way, the target distribution can be computed. Based on the output format of an underlying target tracker, a delta function model or a bi-variate Gaussian model can be used. The target distribution t over an environment is computed as follows:

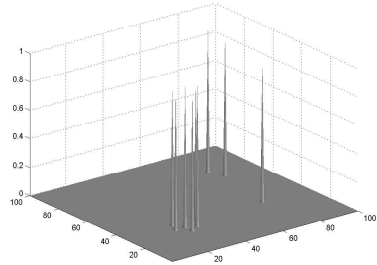
$$t = \sum_i \delta(\mathbf{x}_i) \quad (4.6)$$

$$t = \sum_i N(\mu_i, \Sigma_i) \quad (4.7)$$

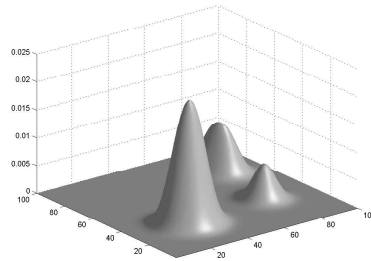
Figure 4.3 (a) shows the target distribution using the delta function model, and Figure 4.2 (b) shows the target distribution using the bi-variate Gaussian model when the positions of targets are as in Figure 4.1.

To define the density estimates, a region boundary R of a unit space must be defined. Two possible models can be used: binary model and Gaussian model. The binary model in Equation 4.8 defines a region boundary with radius r , which is conceptually simple and computationally cheap. The shape of the boundary is shown in Figure 4.4 (a).

$$R(\mathbf{x}) = \begin{cases} 1.0 & \text{if } |\mathbf{x}| < r \\ 0.0 & \text{otherwise} \end{cases} \quad (4.8)$$

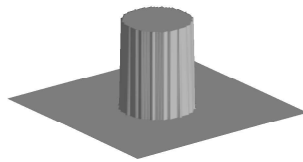


(a) Delta function model

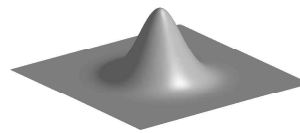


(b) Gaussian model

Figure 4.3: Target distribution model: (a) is preferable when a target tracker returns position estimates only, and (b) is adequate when it returns both position estimates and uncertainty estimates. The positions of targets are shown in Figure 4.1.



(a) Binary region model



(b) Gaussian region model

Figure 4.4: Region models for density computation: (a) is conceptually simple and computationally cheap, but (b) is preferable if a differentiable output is required.

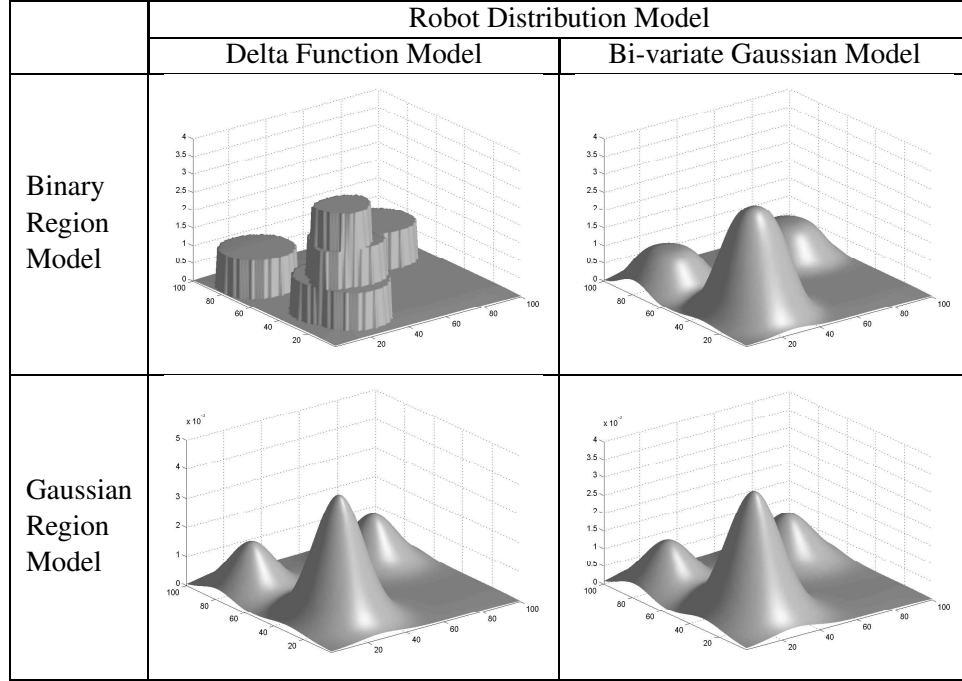


Figure 4.5: Robot density distribution: combinations of different robot distribution models and different region boundary models. The positions of robots and targets are shown in Figure 4.1.

A Gaussian model can be used to define a region boundary when a differentiable output is preferred. The Gaussian distribution is zero-centered and the boundary is determined by a covariance matrix Σ . The shape of a boundary is shown in Figure 4.4 (b).

$$R(x) = N(\mathbf{0}, \Sigma) \quad (4.9)$$

The final density distribution of robots (D_r) or targets (D_t) are computed using convolution of the robot location and region extent:

$$D_r(x, y) = r \otimes R = \int_{-\infty}^{\infty} \int_{-\infty}^{\infty} r(\tau, \rho) R(x - \tau, y - \rho) d\tau d\rho \quad (4.10)$$

$$D_t(x, y) = t \otimes R = \int_{-\infty}^{\infty} \int_{-\infty}^{\infty} t(\tau, \rho) R(x - \tau, y - \rho) d\tau d\rho \quad (4.11)$$

Figure 4.5 and Figure 4.6 show the final density distribution examples with different robot distribution models and region boundary models when the positions of robots and targets are as shown in Figure 4.1.

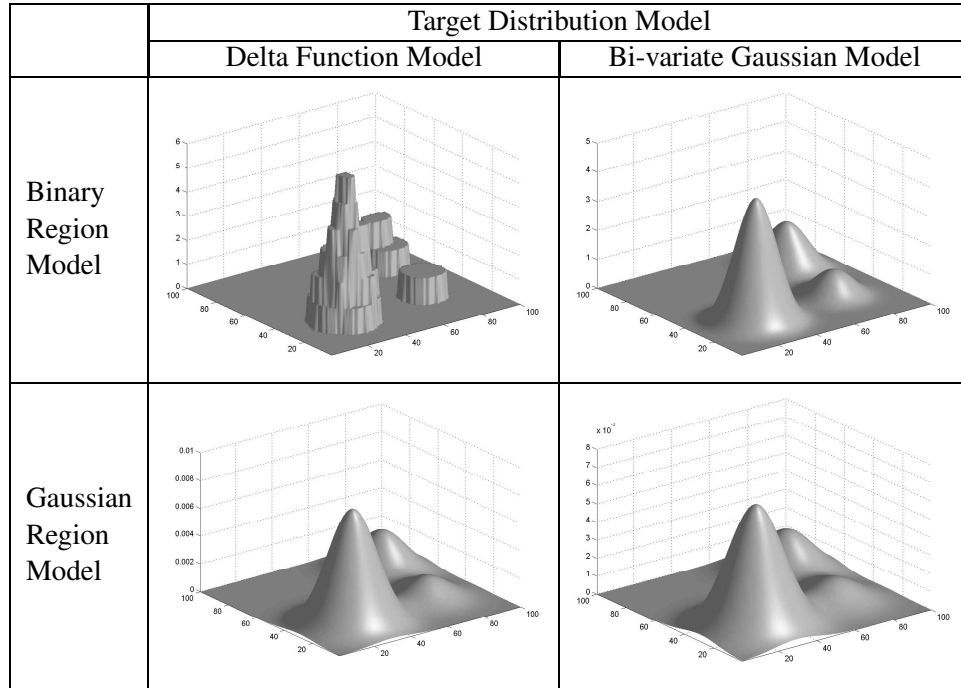


Figure 4.6: Target density distribution: combinations of different target distribution models and different region boundary models.

4.3.2 Urgency Distribution and Utility

Given the distribution of robots D_r and the distribution of targets D_t in a bounded environment, we define the urgency distribution u :

$$u(x, y) = \frac{D_t(x, y)}{D_r(x, y)} \quad (4.12)$$

Figure 4.7 shows the urgency distribution calculated using different models. As shown in Figure 4.1, there are three groups of targets: six targets around at the coordinate $(30, 30)$, two targets around at $(80, 80)$, and a single target at $(75, 35)$. The first two groups are being observed by robots, and those regions have relatively low urgency values as shown in Figure 4.7. However, the last group is not being tracked with any robot, so the urgency value of the region is very high, which means the region requires a robot.

A cost function c_r for each robot can be combined to compute the final utility function for robot control instead of simply using the urgency distribution as an utility function. For example, the cost of motion can be integrated by multiplying a function which is inverse-proportional to a travel distance. Figure 4.8 shows an example of those functions; the inverse cost function for the robot at $(20, 80)$ has a peak at the current position of the robot since the cost of traverse is

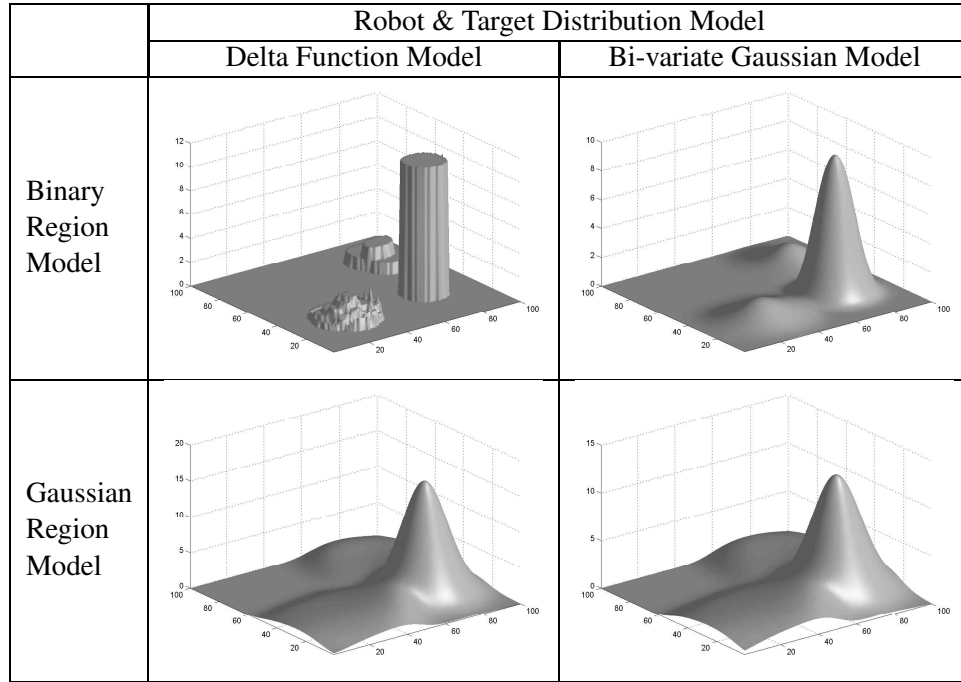


Figure 4.7: Urgency distribution: The urgency values indicate how “urgently” a region should be observed based on robot and target distributions over an environment.

zero, and it decreases as it moves further from the current position because the cost of traverse increases. The final utility distribution function is defined as:

$$U(x, y) = u(x, y) \times \frac{1}{c_r(x, y)} \quad (4.13)$$

It is worth noting that each robot would have a different utility distribution because of the cost function term c_r . Since the urgency distribution u is calculated using the position information of robots and targets, every robot would maintain the same u distribution unless there is failure in communication. However, the different positions of robots cause different costs for a region, and eventually diverse behaviors for robots are generated.

The final utility distribution for the robot at the coordinate (20, 80) is shown in Figure 4.9. Intuitively, the region at the coordinate (75, 35) would attract the robot since it has the highest utility value.

4.3.3 Distributed Motion Strategy

Given the utility distribution, we define two motion strategies. If only local planning is desired, then one possible motor command is a gradient descent method on the utility function as follows:

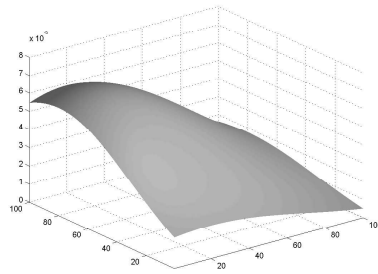


Figure 4.8: Example of an inverse cost function: It has a peak at the current position of a robot since the travel cost is zero, and it decreases as it moves further from the current position because the cost increases.

		Robot & Target Distribution Model	
		Delta Function Model	Bi-variate Gaussian Model
Binary Region Model			
Gaussian Region Model			

Figure 4.9: Utility distribution: The utility distribution of each robot is different from those of others. The distributions in the figure are for the robot at the coordinates (20, 80).

$$\dot{\boldsymbol{x}} = -\nabla U \quad (4.14)$$

If global planning is preferred, then the peak position of the utility distribution can be a goal position:

$$\boldsymbol{x}' = \arg \max_{\boldsymbol{x}} U(\boldsymbol{x}) \quad (4.15)$$

Each robot plans its motion and executes it *independently* in a distributed manner, and there is no explicit negotiation between robots. However, by sharing the position information of robots and targets, these motion plans are coupled.

4.4 Grid Region-Based Approach

The concept of the *Region-based Approach* was described through an example in Section 4.3. However, such conceptual models are not directly applicable to real-world systems because of limited sensor range for target tracking, insufficient computing power for utility distribution evaluation over the environment, etc.

A fine discretization of the *Region-based Approach* is presented in this section, which can be implemented for cooperative tracking in unstructured environments. A grid-based representation is used for the density estimates and the utility distribution, and the region boundaries are determined according to the properties of an underlying target tracker.

4.4.1 Virtual Region Representation and Density Estimates

In order to compute the utility distribution for multi-robot cooperation, the robot density and the target density should be defined first, which subsequently requires the definition of a region boundary. For simplicity, the delta function models in Equation 4.4 and Equation 4.6 are assumed for robot and target distributions, and the binary region model in Equation 4.8 is used for a region boundary.

A virtual region is represented by four parameters: a center position (x, y) , a radius l_r for robot density estimation, and a radius l_t for target density estimation. As shown in Figure 4.10, the radius l_r and l_t are determined according to the sensor range and the field-of-view of a target tracker. For the robot density distribution, a region boundary is defined as follows:

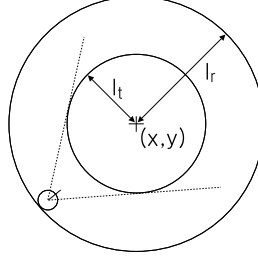


Figure 4.10: Parameterized virtual region: The radius l_r and l_t are determined according to the properties of a tracking sensor.

$$R_r(\mathbf{x}) = \begin{cases} 1.0 & \text{if } |\mathbf{x} - \mathbf{x}_c| < l_r \\ 0.0 & \text{otherwise} \end{cases} \quad (4.16)$$

where \mathbf{x}_c is the center of a region. In a similar way, a region boundary for the target density distribution is defined as follows:

$$R_t(\mathbf{x}) = \begin{cases} 1.0 & \text{if } |\mathbf{x} - \mathbf{x}_c| < l_t \\ 0.0 & \text{otherwise} \end{cases} \quad (4.17)$$

Two density estimates are computed simply as follows:

$$\begin{aligned} D_r(x, y) &= r \otimes R_r(x, y) = \text{the number of robots within a distance } l_r \\ D_t(x, y) &= t \otimes R_t(x, y) = \text{the number of targets within a distance } l_t \end{aligned} \quad (4.18)$$

Each robot broadcasts its current position and the tracked targets' positions, and maintains internal estimates of $D_r(x, y)$ and $D_t(x, y)$ based on the broadcast packets it receives and its own sensor readings. Due to packet loss the estimates may not accurately measure the actual values. Further, the target density values will necessarily be inaccurate because the robots can only count tracked targets. Lastly, both sets of estimates can (and do) vary from robot to robot.

4.4.2 Estimation of the Utility Distribution

Similar to the general *Region-based Approach*, the utility value for every virtual region is defined as in Equation 4.19, where d is the Euclidean distance between the current robot position and the center of a virtual region (x, y) .

$$U(x, y) = \begin{cases} \frac{D_t(x, y)}{D_r(x, y)} \times ic_r(d) & \text{if } D_r \neq 0 \\ D_t(x, y) \times \alpha \times ic_r(d) & \text{if } D_r = 0 \text{ \& } D_t \neq 0 \\ 1.0 & \text{if } D_r = D_t = 0 \end{cases} \quad (4.19)$$

$$ic_r(d) = e^{-\frac{1}{2} \times \left(\frac{d}{\theta_d}\right)^2}$$

The utility computation is not different from the generic version in Equation 4.13 except that it treats the mathematical exceptions (*eg.* infinity and zero divided by zero) separately. The parameter α is a constant to scale the utility value in the case of infinity to a reasonably big value, and the parameter θ_d is a constant to determine the inclination of the inverse cost function ic_r .

There are two implementation issues: (a) how to cope with the unbounded state space, and (b) how to represent the continuous utility distribution $U(x, y)$ efficiently. When an environment is unbounded, then the utility distribution $U(x, y)$ is supposed to be evaluated over the entire space theoretically. However, the effective search space can be limited by the fact that the evaluation is performed based on the detected targets only. In other words, the value of $U(x, y)$ will be a constant when the distance from the position (x, y) to the position of any robot in the system is bigger than a certain threshold, which is $\theta_s = l_e + l_t$ when l_e is the effective range of a tracker. Therefore, the size of the effective search space is proportional to the number of robots in the system.

There are two popular methods to represent a continuous function: grid method and non-uniform (adaptive) sampling. The non-uniform sampling is beneficial when the search space is big and the distribution of function values are concentrated on several areas (*eg.* the entropy of the function is small). For the proposed target-tracking system, the search space is relatively small, and targets can move in and out of the search space quite often. Therefore, a grid method is adopted for the utility distribution representation.

Figure 4.11 shows a snapshot of the utility distribution. Robots are marked with empty circles, and targets are drawn as filled circles. The color of each grid cell represents the utility value; the darker the color is, the higher the utility value is.

4.4.3 Motion Strategy for Cooperative Target Tracking

The motion of each robot is determined in similar way to the original *Region-based Approach*. The utility distribution is updated based on the latest density estimates, and Equation 4.15 is evaluated to search the most urgent region. By changing the parameter θ_d of the cost function

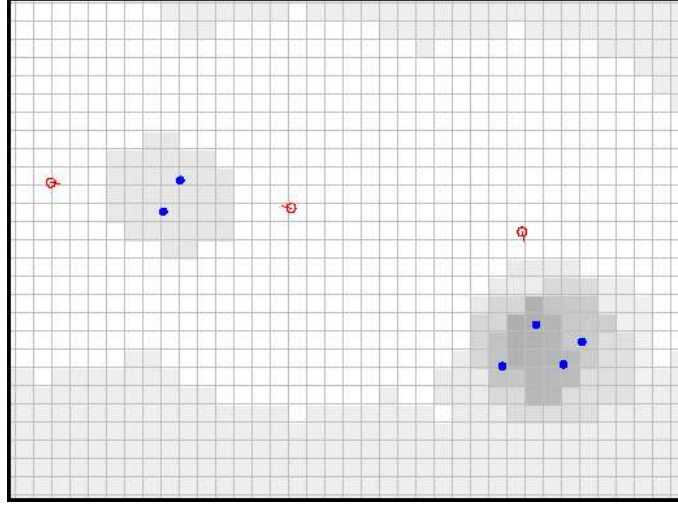


Figure 4.11: Snapshot of the utility distribution: The darker the color of a grid cell is, the higher the utility value of the region is. It is noticed that only the effective search space is evaluated.

$ic_r(d)$, the chance for a robot to select a closer region with smaller utility over a farther region with bigger utility can be controlled.

Even though the utility distribution is evaluated for limited space only, the amount of computation is still intensive because of the high update rate. The motion of each robot can be computed more efficiently by adding an availability checking step. Before updating the utility distribution, each robot checks if it is available to migrate to a more urgent region by evaluating Equation 4.20, where $T(x, y, l_t)$ is the number of targets tracked by the robot in the region $R_t(x, y)$. By checking the availability of a robot in advance, the robot need not evaluate the utility distribution at every cycle, which reduces the computing time.

$$\max_{\forall x, y} \left[\frac{D_t(x, y)}{D_r(x, y)} \times T(x, y, l_t) \right] < \theta_t \quad (4.20)$$

Equation 4.20 was constructed based on the following facts:

- The less targets a region has, the less robots the region requires.
- The more robots a region has, the more robots in that region are free to move to other regions.
- The fewer targets a robot is tracking at a given moment, the less the robot is required to stay in its current region.

θ_t is a parameter that decides how easily a robot would give up tracking the current targets and travel to other regions hoping to find a new, bigger group of targets.

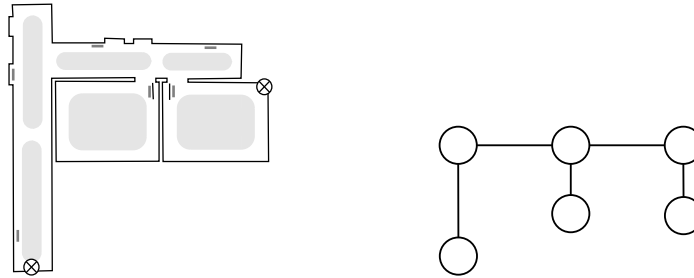


Figure 4.12: Example of a topological map: The environment (on the left) consists of two offices and two long corridors, and the topological map (on the right) can be constructed as a graph.

4.5 Topological Region-based Approach

The *Region-based Approach* can be simplified further by exploiting environmental features. For structured environments (eg. office-type indoor environment), the following assumption can be made:

The environment can be divided into topologically simple convex regions using certain landmarks as demarcaters. Each region is assumed to be simply connected¹. Figure 4.12 shows an example of a topological map shown as a graph. In the topological map, a node corresponds to a region, and a link corresponds to a landmark. For example, the link between two corridor regions may be a corner.

For the *Topological Region-based Approach*, the density estimates and the utility distribution are maintained for nodes on a topological map, which are discrete and sparse. The advantage of this coarse discretization is that the computation for those distribution is very cheap.

Many on-line, topological mapping techniques have been demonstrated in (Choset and Burdick, 1995a,b; Dedeoglu et al., 1999; Dedeoglu and Sukhatme, 2000; Kuipers and Byun, 1991; Kunz et al., 1999; Nagatani and Choset, 1999; Rekleitis et al., 2001; Tomatis et al., 2001), which segment the environment into regions automatically. In this thesis, we focus on the high-level cooperative tracking problem assuming a topological map of the environment is given *a priori*.

4.5.1 Density Estimates on a Topological Map

Given a topological map, every robot independently maintains two density estimates for each node (region). The density estimates are somewhat different from Equation 4.10 & 4.11 or

¹Two regions are connected with a single edge only when they are physically connected such that a robot can traverse from a region to another.

Equation 4.18 defined in the previous sections because the region boundary is determined by the physical structure of an environment and the area of each region is not same anymore. Now, the density estimates in Equation 4.21 & 4.22 are defined as the number of robots or targets in a region normalized by the sensor coverage area of a single robot.

$$D_r(R) = \frac{\text{the number of robots in region } R}{\text{area of region } R / \text{unit coverage}} \quad (4.21)$$

$$D_t(R) = \frac{\text{the number of targets in region } R}{\text{area of region } R / \text{unit coverage}} \quad (4.22)$$

Since the representation of the internal map is coarse enough, we can make a robot remember past observation in order to improve its performance. The target density in Equation 4.22 can be modified as in Equation 4.23, which utilizes the negative number range as a memory.

$$D_t(R) = \begin{cases} -1 & D_t(R) = 0 \ \& \ D_r(R) \neq 0 \\ D_t(R) + \alpha & D_t(R) < 0 \ \& \ D_r(R) = 0 \\ \frac{\text{the number of targets in region } R}{\text{area of region } R / \text{unit coverage}} & \text{otherwise} \end{cases} \quad (4.23)$$

The value of $D_t(R)$ is normally calculated on-board each robot using the third formula of Equation 4.23, but is set to -1.0 when the number of targets in region R is 0 and the number of robots in region R is nonzero *eg.* $D_r(R) > 0$. This explicitly encodes the case when the region is marked as *empty* ($D_r(R) > 0$, $D_t(R) = -1$) as opposed to the case where the region is *unobserved* ($D_r(R) = 0$, $D_t(R) = 0$). Further, when no robots visit region R for a while, $D_t(R)$ is increased slowly over time until it becomes 0, which means that robots forget over time that a region R was explicitly labeled as being empty.

4.5.2 The Coarse Deployment Strategy

The utility distribution for the *Topological Region-based Approach* is defined as similar way to Equation 4.13. Given a distance d from its current position to a region R and an average distance d_{avg} between adjacent regions on the map, the utility value $U(R)$ of a region R is calculated using Equation 4.24. Following the motion strategy rule in Equation 4.15, a robot selects the largest $U(R)$ value, and navigates to the region R using the topological map.

$$U(R) = u \left(D_t(R), D_r(R) \right) \times \frac{d_{avg}}{d}$$

$$u(D_r, D_t) = \begin{cases} \frac{D_t}{D_r} & D_r \neq 0 \\ D_t \times \alpha & D_r = 0 \text{ \& } D_t \neq 0 \\ 1.0 & D_r = D_t = 0 \end{cases} \quad (4.24)$$

$$\alpha = \frac{\text{area of region } R}{\text{unit coverage}} \times \theta_d$$

Equation 4.24 is a formalization of the following ideas:

If there is a region that has targets but does not have a robot, or if there is a region that has more targets than robots, then some robot should move to the region. Otherwise, a robot should move to an unobserved region ($D_r = D_t = 0$) for exploration. θ_d is a parameter that controls how far a robot is willing to travel; for example, by setting θ_d to a small number, a robot is more likely to choose a closer region with less targets over a farther region with more targets, and vice versa.

As explained in Section 4.4.3, the computing time of the utility distribution can be saved by adding the availability checking step. Before updating the utility values of all regions, a robot checks if it is available to migrate to a region which more urgently needs robots. When a robot is tracking T targets in the current region R_c , the robot is said to be available if the inequality in Equation 4.25 is satisfied.

$$\frac{D_t(R_c)}{D_r(R_c)} \times T < \theta_t \quad (4.25)$$

Equation 4.25 was constructed based on the same idea described in Section 4.4.3. θ_t is a parameter that decides how easily a robot would give up tracking the current targets and travel to other regions hoping to find a new, bigger group of targets.

4.5.3 Target Tracking within a Region

The *Topological Region-based Approach* requires one more motion strategy: movements within a region since a region corresponds an space, not a position. Each robot tries to maximize the number of tracked targets within a region. In order to track multiple targets using a camera with limited field of view (FOV), a robot should be positioned close enough not to lose any target, and far enough to keep all targets within its FOV. In order to approach this position, each robot calculates the center of gravity (COG) of the current tracked targets as shown in Figure 4.13. The

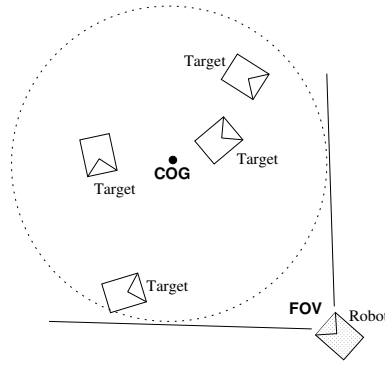


Figure 4.13: Following targets within a region: A robot maintains a proper distance from the center of gravity (COG) of the current tracked targets.

robot attempts to keep at a distance (Equation 4.26) from the COG where d_{max} is the distance between the COG and the target furthest from the COG in the group.

$$distance = \frac{d_{max}}{\sin(FOV/2)} \quad (4.26)$$

4.6 Discussion

Two different levels of simplification of the *Region-based Approach* are presented for the cooperative target tracking using a group of mobile robots. The *Grid Region-based Approach* adopts a grid representation for the utility distribution. This method is efficient in the sense that the best region boundary is selected according to the tracker properties and targets are grouped automatically. On the other hand, the *Topological Region-based Approach* exploits a topological map of an environment, which provides pre-partitioned regions. Since the representation is discrete and sparse, the required computing power is very low. However, this method is valid only for structured environments, and an additional motion strategy (movement within a region) is required. The performance of those two methods is analyzed in the following chapters.

Chapter 5

Experiments in Structured Environments

The problem of tracking multiple anonymous targets in a structured, planar environment using a network of communicating robots and optionally stationary sensors. The *Topological Region-based Approach* described in Section 4.5 is exploited for cooperation among multiple robots. For the performance analysis, three experiments are performed:

1. The *Topological Region-based Approach* is compared to a ‘naive’ local-following strategy in three different environments with varying degree of occlusion.
2. The environment is held constant, and two techniques (*robot density* and *visibility*) for computing urgency distributions were compared.
3. Different combinations of mobile robots and stationary sensors were compared in a given environment.

5.1 System Design and Implementation

Figure 5.1 shows a behavior-based control architecture for the mobile robots, which implements the *Topological Region-based Approach*. The controller consists of three layers: *Motor Actuation Layer*, *Target Tracking Layer*, and a *Monitoring Layer*.

5.1.1 The Motor Actuation Layer

The *Motor Actuation Layer* controls robot deployment; for example, it causes a robot to approach targets, or traverse from one region to another. There are four modules in this layer.

The *RobotMove* module is a repository of basis behaviors (Matarić, 1997), and always performs one of these behaviors as selected by the *RobotDispersion* module. The basis behaviors are *RandomWandering*, *WallFollowing*, *TargetFollowing*, *SpotApproaching*, and *TurningAround*.

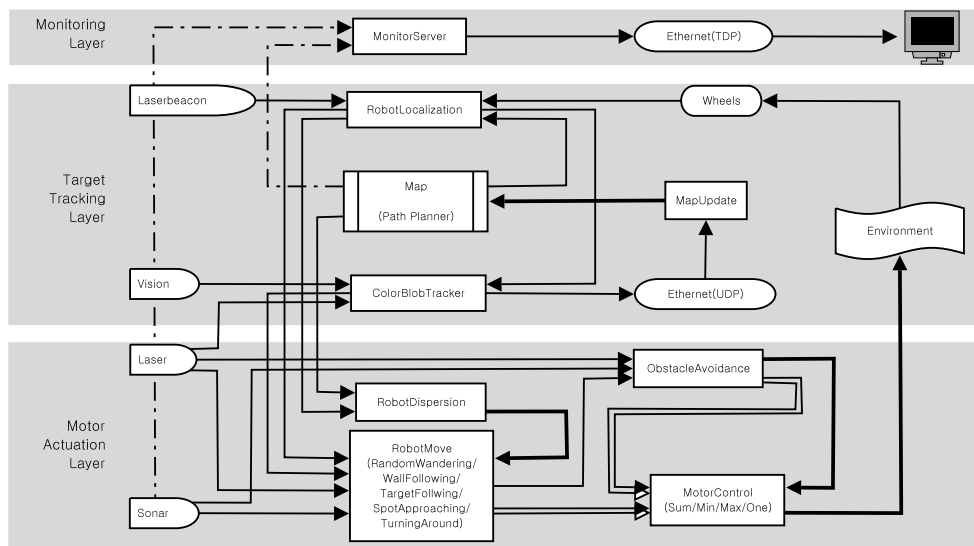


Figure 5.1: Behavior-based robot control architecture: Behaviors are drawn as rectangles, and sensors are shown as half ellipses (read only) or full ellipses (read/write). Thin arrows indicate information flow (a module can share its internal data with other modules), and thick arrows indicate parameter modification (one module can change other modules' behavior). Dashed lines show user-selected debugging information, and double lines emphasize that a behavior generates decoupled motor control commands (one for speed control and one for heading control).

Other than *TargetFollowing* which needs some explanation, the others are relatively standard and self-explanatory. *TargetFollowing* acts differently when a robot uses the robot density (Equation 4.21) for computing the urgency distribution and when it uses the visibility (Equation B.1). In the former case, *TargetFollowing* causes a robot to approach the center of gravity (COG) of all tracked targets (Figure 4.13). It also controls the distance between the robot and the COG based on how much the targets are spread. However, in the latter case, *TargetFollowing* makes a robot approach the COG of only selected targets and keep away from other robots (Figure B.2).

The *RobotDispersion* module disperses robots to regions. It checks a robot's availability by accessing the internal map (*Map*), and drives the robot to the most urgent region by following a path generated by *Map* module.

The *MotorControl* module generates actual motor control signals (Speed & Turnrate) based on input signals from other modules. It has four different modes: *Sum*, *Min*, *Max*, and *One*. All inputs are integrated in *Sum* mode, or a single, specified input is used in *One* mode; minimum/maximum inputs are selected in *Min/Max* mode.

The *ObstacleAvoidance* module is for safe navigation. It acts differently when a robot is tracking targets and when it is not. It executes only speed control when a robot is tracking

targets, and leaves turnrate control to *RobotMove* (more specifically *TargetFollowing*). However, it regulates both speed and turnrate control when a robot is not tracking a target.

5.1.2 The Target Tracking Layer

The modules in the *Target Tracking Layer* detect targets, estimate their positions, and interchange this information among robots so that each robot can compute the density estimates defined earlier.

The *RobotLocalization* module keeps track of a robot's position. Since a robot calculates the positions of tracked targets based on its local coordinate system, knowing the robot's position is important for accurate target position estimation. This module estimates the robot's position based on odometry all the time, and compensates drift error whenever it sees laser beacons¹ which are disseminated in the environment at region boundaries. Given the global positions of the laser beacons and distance/bearing information to them, the *RobotLocalization* module can estimate the position and heading of a robot very accurately, and can correct odometry error.

The *ColorBlobTracker* module detects targets of certain colors, and calculates their positions. It uses a camera to detect targets and to calculate bearing to them, and uses a laser rangefinder to measure the distance to the targets. More details about the tracker can be found in (Jung and Sukhatme, 2001). The positions of targets in the robot's local coordinates are saved for the *TargetFollowing* behavior, and the positions in global coordinates are broadcast over the wireless network at the speed of 10 Hz.

The *MapUpdate* module receives the broadcast packets, and updates density information in the *Map* module. Each target is identified by its global position; if the distance between two target positions is smaller than the twice length of a robot body, the two targets are assumed as a single target. The *Map* module is a passive data storage; all its contents are updated by the *MapUpdate* module. However, it has a functionality of a path planner; it can generate topological paths from one region to a specified goal region when there is a request from other modules.

5.1.3 Monitoring Layer

The *Monitoring Layer* is not directly related to the controller, but it provides a convenient means to observe the internal status of the controller during operation. Since the bandwidth of the wireless network is limited, each robot sends its internal information only when there is a request

¹The laser beacon (Howard et al., 2001) is a simple bar-code constructed using strips of retro-reflective paper. Based on the reading from a SICK laser rangefinder, a robot can compute the ID, range, bearing, and orientation for each visible beacon.

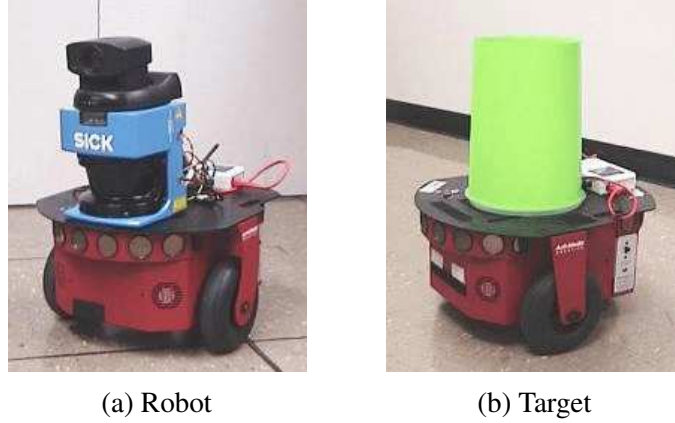


Figure 5.2: Configurations for robots and targets: Pioneer robot is equipped with a SICK laser rangefinder and a Sony PTZ camera, and each target was a Pioneer robot carrying a bright-colored cylinder

from an external monitoring program. Currently, this layer is used for debugging only, but it can be used for inter-robot communication for future extension.

The *MonitorServer* module is a thread-based server program; it always listens to a specified port, and sends selected internal data of other modules when there is a request. The module can serve more than one client at a time.

5.2 Experimental Setup

To evaluate our approach, we performed experiments with ActivMedia Pioneer DX-2 robots and the *Player/Stage* software platform. Pioneer robots equipped with a SICK laser rangefinder and a Sony PTZ camera were used for tracking, and each target was a Pioneer robot carrying a bright-colored cylinder (see Figure 5.2).

Tracking performance was evaluated using Equation 5.1. Following (Parker, 1997) we define the Observation as

$$Observation = \sum_{t=0}^T \frac{n}{N} \times \frac{1}{T} \times 100 \quad (5.1)$$

where N is the total number of targets, n is the number of targets being tracked at time t and the experiment runs over time T .

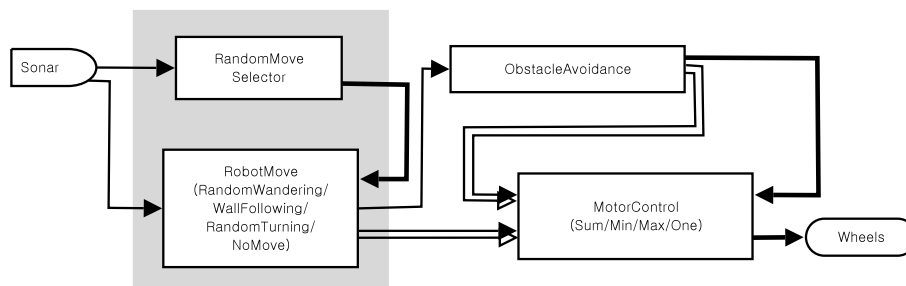


Figure 5.3: System architecture for targets: A target shows four different behaviors (wander, follow walls, turn in place, or stop) in random combination.

5.2.1 Target Modeling

Pioneer robots were used as moving targets. Each target robot uses sonar sensors for obstacle avoidance, and carries a bright-colored cylinder that is easily detected by a vision system. As shown in Figure 5.3, targets have four different behaviors: *Random-Wandering*, *Wall-Following*, *Random-Turning*, and *No-Move*. Each behavior is chosen randomly with probabilities (0.3, 0.3, 0.2, 0.2) in order. This target model showed sufficiently unpredictable, complex movement during experiments.

5.2.2 Environment Complexity

After having observed several simulations, we realized that the characteristics of the environment affect the system performance. The shape of the environment, in particular how obstructed it is, seems to be significant. In order to investigate this correlation between the *Topological Region-based Approach* and characteristics of environment, we chose three distinct environments shown in Figure 5.4. The first environment, *Corridors*, consists of long, narrow regions which cause many occlusions. Each region is narrow enough that a single target may cause serious occlusion to the trackers. The second environment, *Concave*, consists of several relatively big regions with few occlusions. The last environment, *Convex*, is a single empty space which has no occlusion at all. Occlusions can be caused only by targets or other robots. The areas of these three environments are equal.

A formal approach to analyze the complexity of environment models has been introduced in (Cazals and Sbert, 1997). The basic idea of the approach is to generate uniformly distributed random rays, and to compute statistics such as how often rays intersect with models, how long truncated segments are, etc. Various characteristics about 3D models can be inferred from these

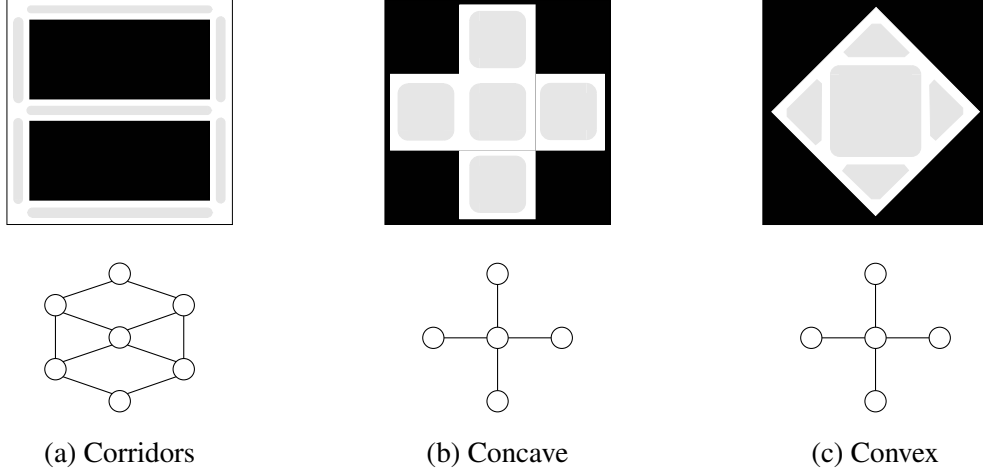


Figure 5.4: The simulation environments: The black regions are occupied and the rest is free space. The associated topological maps are shown as graphs. (a) *Corridors* consists of long, narrow regions which cause many occlusions. (b) *Concave* consists of several relatively big regions with few occlusions. (c) *Convex* is a single empty space which has no occlusion at all.

statistics. We utilize this approach in order to measure the complexities of our planar environments.

As explained in (Cazals and Sbert, 1997), two end-points of rays must be selected from the *circumcircle* of environment images for uniform distribution, not from the bounding box. In order to meet this restriction, two angles (θ_1, θ_2) were randomly generated, and the two end-points (x_1, y_1) and (x_2, y_2) were computed as follows when r is the radius of the circumcircle:

$$x_1 = r \times \cos(\theta_1), y_1 = r \times \sin(\theta_1)$$

$$x_2 = r \times \cos(\theta_2), y_2 = r \times \sin(\theta_2)$$

If a ray did not intersect with the bounding box of environment images at all, the ray did not count.

Table 5.1 shows the statistics of the three environments. The environments with several targets present were also tested in order to investigate how the complexities change when there are robots/targets in the environments. The targets were evenly distributed in regions. In Table 5.1, p_0 is the probability that a ray does not intersect with any objects, *eg.* walls, robots, and targets. en_{int}^G is the average of the number of intersection points, and σen_{int}^G is its standard deviation. μCL is the average of the length of free lines², and σCL is its standard deviation. Especially, p_0

²Free lines are the segments of rays that divided by intersection points. The lengths of the free lines are normalized with the longest free line.

Environment	# targets	# rays	p_0	en_{int}^G	σen_{int}^G	μCL	σCL
Corridors	0	10,000	0.3003	1.9552	1.5201	0.2714	0.2438
Corridors	2	10,000	0.2963	2.0394	1.6076	0.2657	0.2445
Corridors	4	10,000	0.2901	2.1212	1.6646	0.2596	0.2422
Corridors	6	10,000	0.2876	2.1998	1.7273	0.2555	0.2432
Corridors	8	10,000	0.2849	2.2784	1.8201	0.2509	0.2413
Concave	0	10,000	0.7600	0.4800	0.8542	0.4678	0.2798
Concave	2	10,000	0.7260	0.5738	0.9600	0.4478	0.2826
Concave	4	10,000	0.6784	0.7140	1.0983	0.4265	0.2852
Concave	6	10,000	0.6331	0.8188	1.1447	0.4131	0.2853
Concave	8	10,000	0.6015	0.9082	1.1995	0.3992	0.2829
Convex	0	10,000	1.0000	0.0000	0.0000	0.5639	0.2462
Convex	2	10,000	0.9406	0.1196	0.4776	0.5301	0.2601
Convex	4	10,000	0.8800	0.2510	0.6950	0.5057	0.2687
Convex	6	10,000	0.8338	0.3678	0.8613	0.4785	0.2724
Convex	8	10,000	0.8003	0.4688	0.9985	0.4594	0.2730

Table 5.1: Complexity of the environments as a function of number of targets: Only targets are included for the complexity analysis because robots are part of the tracking system, not part of the environment. However, since a robot has the same size with a target, the result can be interpreted such as the number of targets indicates the number of objects including robots.

is a nice indicator showing how much occlusion an environment has, and μCL can be an indicator showing how big (wide) each region is.

As expected, *Corridors* showed small p_0 and μCL , which means it has significant occlusion and its regions are narrow. On the other hand, p_0 of *Convex* was big since it has little occlusion. The μCL values of both *Concave* and *Convex* were big because their regions are wide. Needless to mention, the more targets, the higher complexity.

5.2.3 Experiment Design

Three experiments were performed with various configurations. Two of them were performed using the *Stage* simulator, and the third experiment was performed using *Pioneer DX-2* robots.

5.2.3.1 Region-based versus Local-following Strategy

The *Topological Region-based Strategy* was compared with a *Local-following Strategy*. The *Topological Region-based Strategy* uses the system described in Section 6.1, and the *Local-following Strategy* uses the same architecture without the *RobotDispersion* module. The *Local-following Strategy* still tries to maximize the number of tracked targets in the current region by

maintaining a proper distance from a group of targets as explained in Figure 4.13. The best scenario for the *Local-following Strategy* would be that many targets gather in an open space and stay in a large, circle-shaped group; a single robot would be able to keep track of most of the targets in the group. The worst scenario for the *Local-following Strategy* would be that all robots track the same single target and the rest of targets stay away from the target being tracked; since robots never give up the current tracked target, they would never leave the current region to move to other regions which contain other targets. On the other hand, the *Region-based Strategy* causes a robot to relinquish tracking the current tracked target to explore other regions when there are more than enough robots in the current region; therefore, the worst scenario would never happen. The purpose of this comparison is to measure if the map-based coarse control causes an improvement in tracking performance.

5.2.3.2 Robot Density versus Visibility

Two variants of the *Topological Region-based Approach* are compared. With the *Robot Density*, a robot tracks all targets in its sensing range. However, when robots get too close to each other, the overall performance might reduce. On the other hand, with *Visibility* described in Appendix B, a robot covers a wider area within a region by keeping away from other robots, but this may result in the loss of some targets in the process of receding.

In order to perform experiments with various configurations and minimize the effect of unnecessary factors, the *Stage* simulator is used with the *Corridors* environment shown in Figure 5.4 (a). Thus this experiment does not vary the environment.

5.2.3.3 Mobile Robots versus Embedded Sensors

Another interesting issue in multi-target tracking using multiple sensors is whether adding a mobile sensor (*eg.* a mobile robot) is always more helpful to improve tracking performance compared to adding a stationary environment-embedded sensor (*eg.* a security camera). Each sensor has its own advantages. For example, a mobile sensor can cover wider area over time, and can adapt to targets' movement patterns. On the other hand, a fixed sensor can be installed at the best position depending on the environments, and it causes less interference.³

Since we wanted a realistic environment for this test, the experiments were performed using real robots on the second floor of our Computer Science Building. Figure 5.5 shows the map of the floor and its topological map; it consists of two offices and two long corridors. The figure also

³Actual cost of mobile robots and fixed sensors is not considered for this comparison since we only focus on the performance of cooperative tracking strategies using heterogeneous sensors.

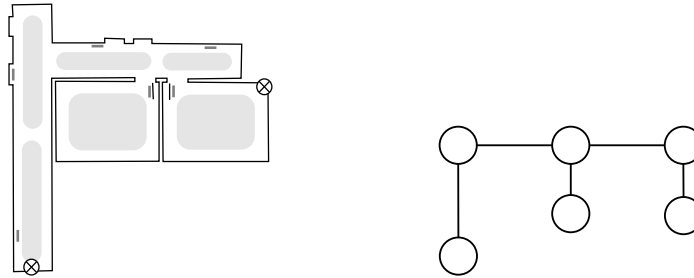


Figure 5.5: Environment for real-robot experiments: It consists of two offices and two long corridors. The laser beacons are shown as dark gray, thick lines on the walls, and the position of stationary sensors are marked by \otimes symbols.

shows the positions of the laser beacons (dark gray, thick lines) and stationary sensors (\otimes marks). In this study the environment and control strategy were held constant and the ratio of the mobile to stationary trackers was varied.

5.3 Experimental Results

5.3.1 Region-based versus Local-following Strategy

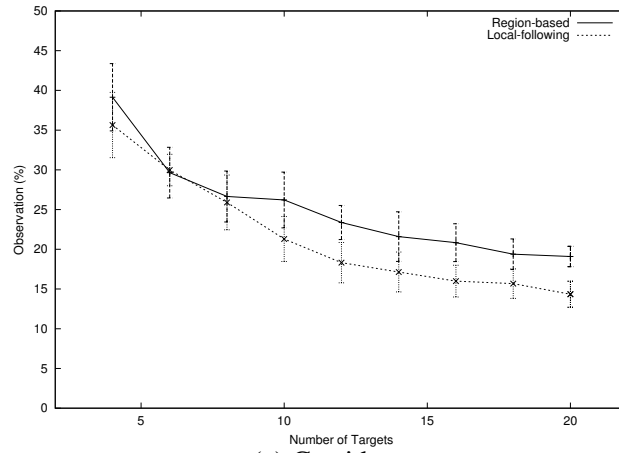
The simulations were performed with various configurations in three different environments. We fixed the number of robots at 2, and changed the number of targets from 4 to 20 in steps of 2. Each configuration ran for 10 minutes a total of 9 times, and the average performance was taken as the final result. The experimental results are shown in Figure 5.6.

5.3.2 Robot Density versus Visibility

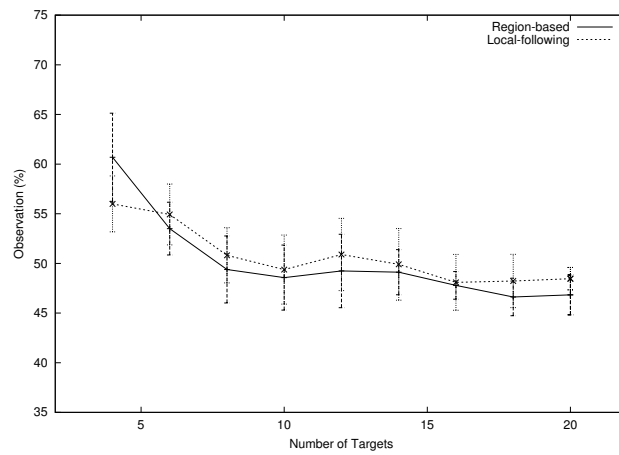
The simulations were performed with various configurations using the *Corridors* environment. We fixed the number of robots at 2, and changed the number of targets from 4 to 20 in steps of 2. Each configuration ran for 10 minutes a total of 9 times, and the average performance was taken as the final result. The result is shown in Figure 5.7.

5.3.3 Mobile Robots versus Embedded Sensors

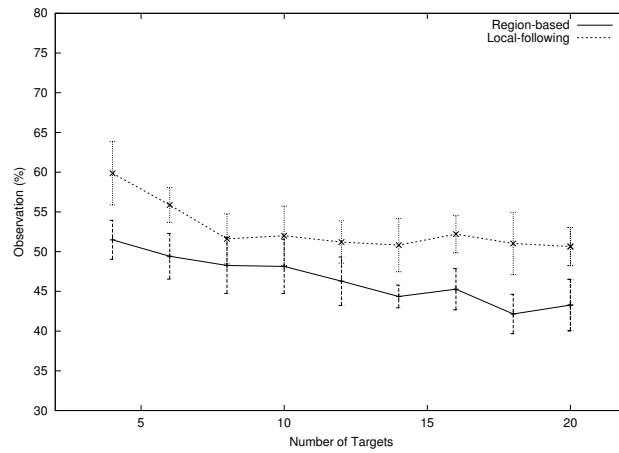
We fixed the number of targets at 4, and used a total of 2 sensors in three different combinations: with only two stationary sensors, with one stationary sensor and one mobile robot, and with two mobile robots. Each configuration was tested over 3 trials, and each trial ran for 10 minutes. The average performance is shown in Figure 5.8. When the robots were used, we performed the experiment twice, using both the *Region-based Strategy* and the *Local-following Strategy*.



(a) Corridors



(b) Concave



(c) Convex

Figure 5.6: Simulation results comparing the performance of the two strategies: The number of robots was fixed at 2, and the number of targets varied from 4 to 20 in steps of 2.

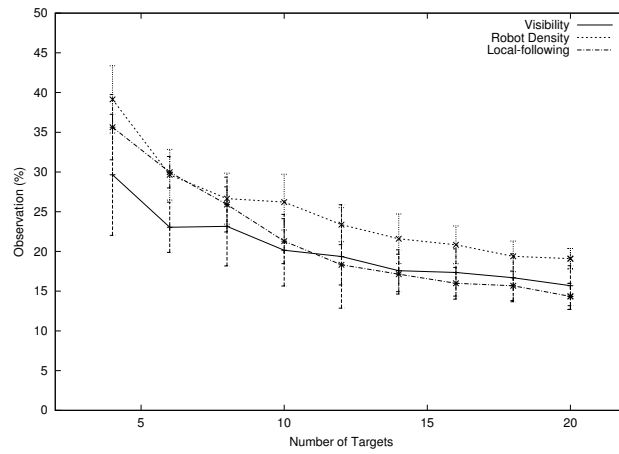


Figure 5.7: Performance with visibility maximization: Three strategies were compared (Region-based strategy with visibility maximization, Region-based strategy with robot density, and Local-following strategy) in the *Corridors* environment. The number of robots was fixed at 2, and the number of targets varied from 4 to 20 in steps of 2.

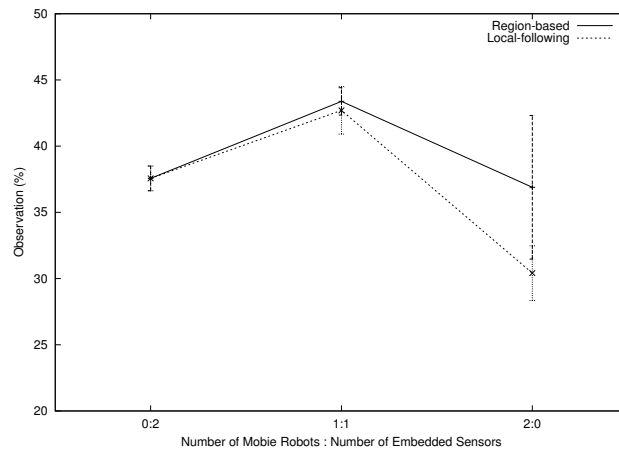


Figure 5.8: Performance of the real-robot system: The number of targets was fixed at 4, and a total of 2 sensors were used in three different combinations (with only two stationary sensors, with one stationary sensor and one mobile robot, and with two mobile robots). The experiment was performed on the second floor of our Computer Science Building shown in Figure 5.5.

# targets	Corridors	Concave	Convex
4	0.112957	0.022510	0.000117
6	0.808498	0.334473	0.000120
8	0.660541	0.369265	0.062597
10	0.007183	0.638818	0.046621
12	0.000549	0.378994	0.003367
14	0.006264	0.608437	0.000124
16	0.000445	0.786089	0.000042
18	0.001258	0.184465	0.000059
20	0.000008	0.062607	0.000093

Table 5.2: Significance values from T-test as a function of number of targets and environment characteristic

5.4 Discussion

5.4.1 Region-based versus Local-following Strategy

In the *Corridors* environment, the *Region-based Strategy* showed better performance, especially when the number of targets was large. Since the regions are narrow and many occlusions are caused, it is almost impossible for a single robot to track more than two targets at a time, which means cooperation among robots is indispensable. On the other hand, the performance of the *Region-based Strategy*, in the *Convex* environment, was not as good as that of *Local-following Strategy*. This can be explained by the fact that a robot is able to track targets in other regions without traversing to those regions in the empty environment because there is zero occlusion. This benefit is maximized for the *Local-following Strategy*, but not for the *Region-based Strategy*. Both strategies showed almost the same performance in *Concave*, whose shape causes a small amount of occlusion.

We performed a t-test with each data points pair in order to see if the results from the two strategies show significant difference statistically. Table 5.2 shows the significance values of the t-test; a small number implies that the two distributions are statistically different. As expected, the significance values of *Concave* were big, and those of *Corridors* and *Convex* were small.

The simulation results show a strong correlation between robot coordination strategies and environment shape. The data in Figure 5.6 suggest that in environments with a low value of p_0 , the *Topological Region-based Approach* out performs the *Local-following Strategy*, and in environments with a high value of p_0 , the reverse is true. However, there are unobserved factors which might be critical to the overall performance, *eg.* region decomposition. The *Topological Region-based Approach* may perform differently when an environment is decomposed into few big regions and when the same environment is divided into many fine regions. Also, the region

# targets	vs Robot Density	vs Local-following
4	0.007200	0.067867
6	0.000737	0.000077
8	0.114616	0.217457
10	0.008551	0.551933
12	0.117852	0.676290
14	0.013156	0.743729
16	0.020076	0.300305
18	0.049254	0.433392
20	0.003620	0.223343

Table 5.3: Significance values from T-test as a function of number of targets and different strategies

decomposition method may have to be varied depending on environment shape; for instance, region size should be small when the complexity of an environment is high, and vice versa. We plan to investigate these issues in future work.

5.4.2 Robot Density versus Visibility

As shown in the t-test result (Table 5.3), the *Topological Region-based Approach* using the *Visibility* did not show significant difference from the *Local-following Strategy*. There are two possible explanations for this.

First, the coverage estimation method might have been inappropriate. Because of lack of global, geometrical information and real-time requirement, simple approximation methods were utilized as much as possible. For example, each sensor’s coverage was computed by integrating real laser readings, but a single simplified sector was used for overlap computation. Also, small error was ignored. For instance, overlap was computed for all possible pairs of robots within a region; when the coverage of three robots (A , B , and C) are overlapped, the coverage intersection $A \cap B \cap C$ is subtracted once more unnecessarily and never compensated.

Second, the visibility maximization method described in Appendix B assumes that tracking sensor is omni-directional, which is not valid in both simulation and real robots. In the current visibility maximization method, when a robot detects other robots, it abandons tracking targets which are positioned closer to the other robots. By doing this, robots can keep distance from each other without explicit communication. In Figure B.2 (c) this method works properly since the upper robot is facing down. However, if the upper robot were facing up, the lower robot would still move same and the other two targets would not be tracked anymore. This problem is caused because the current tracking sensor cannot detect other robots’ heading.

It is expected that better implementation of visibility maximization method would improve its overall performance.

5.4.3 Mobile Robots versus Embedded Sensors

The general tracking performance in the real-robot experiments was not as good as that in the simulation. There are several explanations. First, the effective range of the real vision system (around 4.5m) was much shorter than the range of the simulated one (8m). Also, the field of view (FOV) of the real camera (90 degrees) was not as wide as the FOV of the virtual camera (120 degrees). Second, the environment for the real-robot experiments was much more complex; for example, the connection between offices and corridors (doors) was narrow enough to cause the robots difficulties. Lastly, the odometry error of the real robot was larger, and caused unfavorable effects on navigation; for example, it took longer to traverse from a region to another region.

In case of using two stationary sensors, the performance depends on targets' movement. As shown in Figure 5.8, the standard deviation was small ($\pm 2\%$), which signals that the targets spread out evenly over the environment. When a mobile robot was used together with an embedded sensor, the overall performance was higher than any other cases. As shown in Figure 5.9 (a), the robot was able to position itself properly to track multiple targets, and also able to follow the targets continuously. However, when only two robots were used, the performance was worse than the previous cases, especially with the *Local-following strategy*. Since two robots moved independently to follow targets, they often ended with following the same target, as shown in Figure 5.9 (b). That worst case was observed less often when the system used the *Region-based Strategy*.

Although the case of using a mobile robot and an embedded sensor together showed the best performance, more research on this topic will be necessary to come to a firm conclusion, *eg.* larger-scale experiments with more combinations.

5.4.4 Summary

In this chapter, a mobile sensor network that is able to track multiple targets effectively is presented. The proposed *Topological Region-based Approach* attempts to solve the sensor coordination problem without explicit negotiation among sensors by exploiting a topological map. All mobile sensors maintain utility information independently, and re-position themselves based on that information. The *Topological Region-based Approach* has been implemented with a behavior-based system which is fully distributed and scalable. Through intensive simulations and real-robot experiments, the *Topological Region-based Approach* was shown to perform better than a



(a) 1 robot tracking 2 targets



(b) 2 robots tracking 1 target

Figure 5.9: Tracking examples: (a) shows the favorable case which observed more often when the *Region-based Strategy* is used. (b) shows the worst case which observed more often when the *Local-following Strategy* is used.

naive approach (used as a baseline for comparison) when the environment contains significant occlusion. A simple metric for measuring the degree of occlusion was used, based on the average mean free path of a random line segment drawn in the environment.

The experiments open up two new lines of research, which suggest that (a) an optimal ratio of robots to stationary sensors may exist for a given environment with certain occlusion characteristics, and (b) an optimal ratio of mobile to stationary sensors may exist for a particular environment.

There is an open problem to be investigated in the future. The relationship between our *Topological Region-based Approach* and the region decomposition method (responsible for the structure of the topological map) should be clarified. We assumed, in this work, that the topological map for an environment is given *a priori*, and focused on the relationship between the robot coordination method and the structure of the environment. However, the topology of the decomposed regions may be a critical factor in the overall tracking performance.

Chapter 6

Experiments in Unstructured Environments

6.1 System Design and Implementation

For most surveillance or security applications, motion may be the most interesting feature to track. Therefore, we designed a multi-robot system that tracks and reports the positions of moving objects in outdoor environments. The *Grid Region-based Approach* described in Section 4.4 was utilized for the cooperation among robots. The system architecture is shown in Figure 6.1. The system consists of four components: motion tracking, localization, cooperative motion planning, and navigation.

6.1.1 Motion Tracker

The approach to motion tracking using a single camera on a mobile robot is described in Chapter 3. The tracking results (the positions of moving objects in a local coordinate system) and the tracker information (the robot pose in the global coordinate system) are broadcasted for cooperation over the wireless network.

6.1.2 Localization

All robots share a global coordinate system for multi-robot cooperation, which requires a global localization. Unlike the indoor case, GPS (Global Positioning System) is available outdoors. Combination of a differential GPS and an IMU (Inertial Measurement Unit) provides full pose (x, y, α) correction. The Extended Kalman Filter (Welch and Bishop) and the Unscented Kalman Filter (Julier and Uhlmann, 1997) are implemented for stable pose estimation.

The state vector is defined as

$$\mathbf{x} = [x \ \dot{x} \ y \ \dot{y} \ \alpha \ \dot{\alpha}]^T \quad (6.1)$$

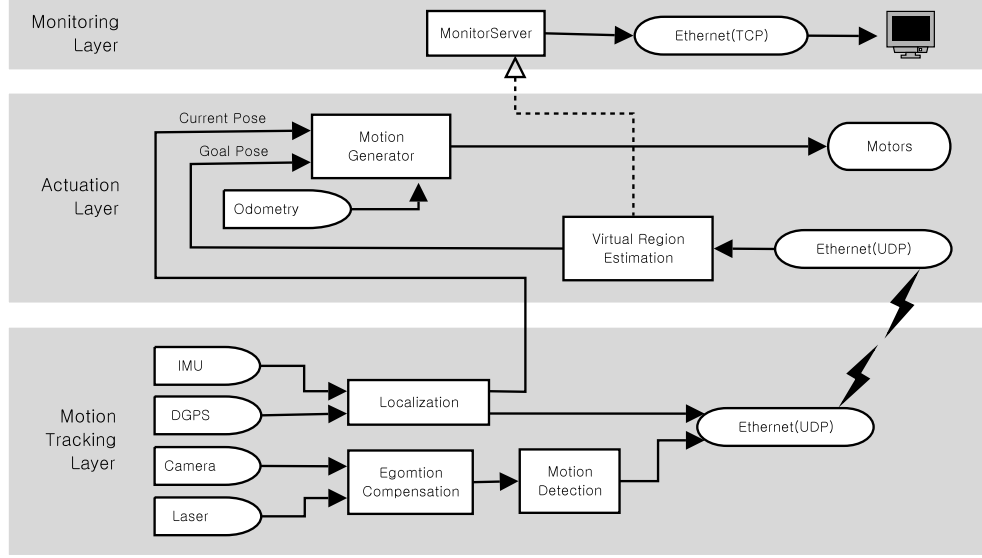


Figure 6.1: System architecture for *Grid Region-based Approach*: The system consists of four components: motion tracking, localization, cooperative motion planning, and navigation.

and the user input vector is defined as

$$\mathbf{u} = [v_t \ v_r]^T \quad (6.2)$$

when v_t is the translational velocity and v_r is the rotational velocity. The dynamics equations are

$$\begin{aligned} x^{t+1} &= x^t + \Delta t \times \dot{x}^t && + w_0^t \\ \dot{x}^{t+1} &= v_t^t \times \cos(\alpha + \Delta t \times v_r^t) && + w_1^t \\ y^{t+1} &= y^t + \Delta t \times \dot{y}^t && + w_2^t \\ \dot{y}^{t+1} &= v_t^t \times \sin(\alpha + \Delta t \times v_r^t) && + w_3^t \\ \alpha^{t+1} &= \alpha^t + \Delta t \times \dot{\alpha}^t && + w_4^t \\ \dot{\alpha}^{t+1} &= v_r^t && + w_5^t \end{aligned} \quad (6.3)$$

and the measurement vectors are defined as

$$\mathbf{z}_{gps} = [x \ y]^T + \mathbf{v}_{gps} \quad (6.4)$$

$$\mathbf{z}_{imu} = [\alpha] + \mathbf{v}_{imu} \quad (6.5)$$

when w , \mathbf{v}_{gps} , and \mathbf{v}_{imu} are noise terms.

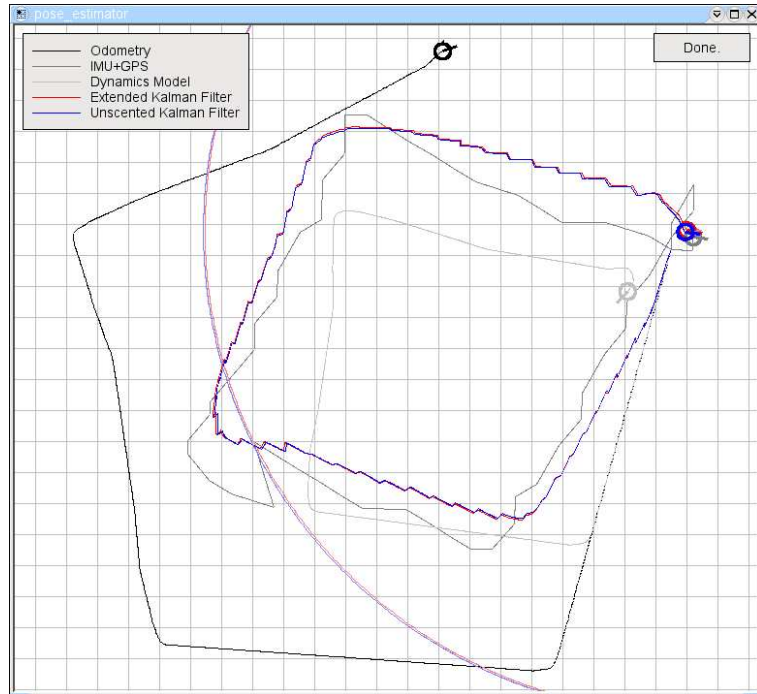


Figure 6.2: Robot localization using Kalman filters: A robot moves along a rectangular route and comes back to the starting position.

Figure 6.2 show the output of Kalman filters. The robot moves along a rectangular route and comes back to the starting position. The estimation with odometer alone shows a serious drift error, and the estimation with IMU and DGPS also shows big jumps in the middle. The dynamic model shows relatively better the pose estimation result, but it fails to close the loop because of accumulated errors. The output of the Kalman filters shows reliable pose estimation; the difference between the results of EKF and UKF was infinitesimal.

6.1.3 Cooperative Motion Planning

The *Grid Region-based Approach* is utilized for cooperative motion planning. The motion trackers on each robot broadcasts its global pose and detected target positions over the wireless network. Each robot *independently* collects those broadcasted messages, and maintains the global position information of robots and targets in the environment. Based on the latest position information, each robot determines if it is available to migrate to other regions using Equation 4.20. Once the robot decides to move, it searches for the most urgent region in an environment using Equation 4.19, and sets the center of the region as a goal position.

6.1.4 Navigation

Given the current robot pose (from the *Localizer* module) and the goal position (selected by the *Generalized Region-based Approach*), a robot should be able to perform point-to-point, safe navigation. In a structured indoor environment, wall-following behavior can be a good navigation mechanism since the environment provides basic guidance from a region to another. However, in an outdoor environment, some other type of local navigation algorithm is required to work without any environmental support.

VFH+ (Vector Field Histogram +) (Ulrich and Borenstein, 1998) algorithm is implemented for point-to-point navigation. VFH+ algorithm provides a natural way to combine a local occupancy grid map and the potential field method, and the dynamics and kinematics of a mobile robot can be integrated to generate an executable path. In addition, the robot's motion property (eg. goal-oriented, energy-efficient, or smooth-path) can be controlled by changing the parameters of a cost function.

Both translational and rotational velocities are controlled by the VFH+ algorithm until the distance between the robot position and the goal position is bigger than l_r . Once a robot is positioned at the distance l_r from a goal position, then only rotational velocity is controlled by the VFH+ algorithm while a translational velocity remains zero. In this manner, a robot would stay close enough not to lose any target, and far enough to keep all targets within its FOV.

The snapshot of the VFH+ algorithm is shown in Figure 6.3. The picture shows a local grid map (9m x 9m) in the robot's coordinate system, and the green dot indicates a goal position. The sectors around the robot show the polar histogram; the shorter the sector is, the higher chance the direction is open.

6.2 Experimental Setup

The performance of the *Grid Region-based Approach* was studied by inspecting the changes of utility distribution caused by the position changes of robots and targets in a simulated environment. The environment was an empty, unbounded space, and there were three robots and ten moving targets in it. The target motions were random, and the grid size was fixed to 1 meter for the urgency function representation.

The *Player/Stage*¹ software platform was used for simulations. *Player* (Gerkey et al., 2001) is a server and protocol that connects robots, sensors and control programs across the network.

¹*Player* and *Stage* were developed jointly at the USC Robotics Research Labs and HRL Labs and are freely available under the GNU Public License from <http://playerstage.sourceforge.net>.

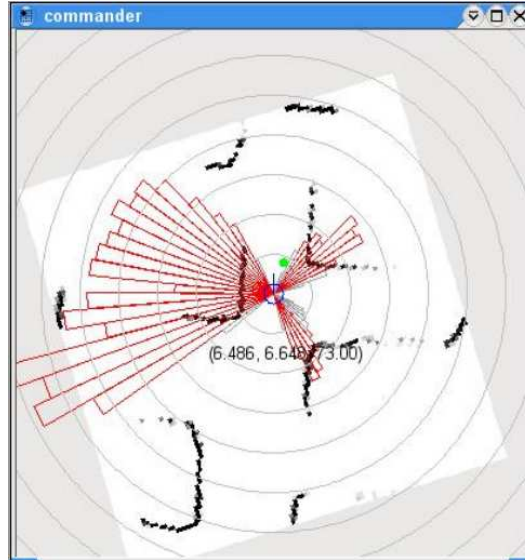


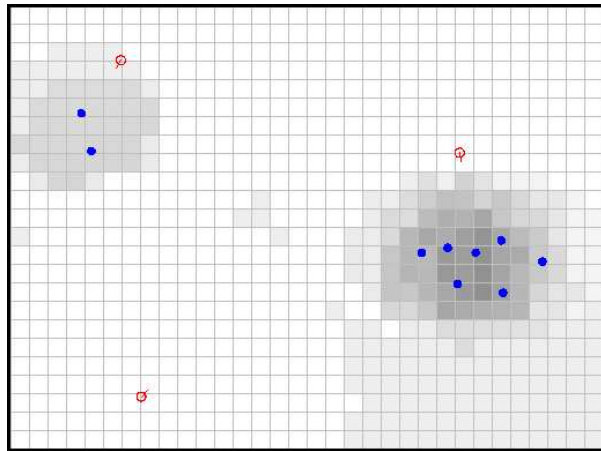
Figure 6.3: Navigation using the VFH+ algorithm: The sectors around the robot show the polar histogram, which means that the shorter the sector is, the higher chance the direction is open.

Stage (Vaughan, 2000) simulates a population of Player devices, allowing off-line development of control algorithms.

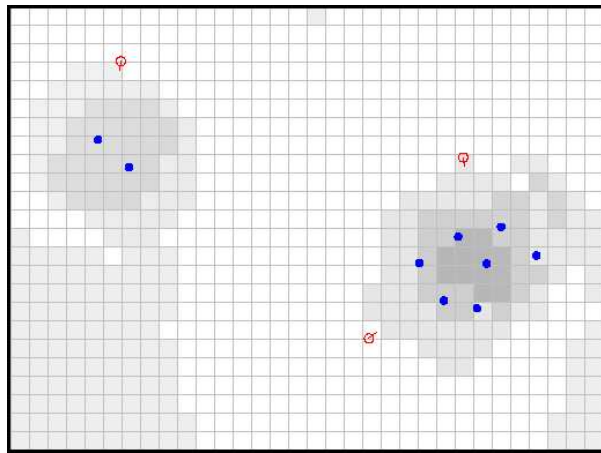
6.3 Experimental Results

Figure 6.4 shows how a robot (on the bottom-left) determines a goal position according to an estimated utility distribution. The gray-scale of each grid indicates its utility value estimated by the robot; the darker the color is, the higher the utility value is. It is obvious in Figure 6.4 (a) that the robot selected the center of the targets on the right as a goal position because there is a peak of the utility distribution. In Figure 6.4 (b), it is clearly shown that the utility distribution becomes balanced after the robot participated in tracking the group of targets on the right.

A switching-region behavior is shown in Figure 6.5. The center robot was tracking the group of targets on the left initially as shown in Figure 6.5 (a). However, when the robot on the right discovers more targets, the utility distribution estimated by the center robot skews to the right (Figure 6.5 (b)). As a result, the center robot migrates to help tracking the group of targets on the right, and the final urgency distribution is shown in Figure 6.5 (c). It should be clarified that the utility distributions shown in Figure 6.5 were the estimations performed by the robot in the center. Because of the function $f(d)$ in Equation 4.19, the urgency estimation of each robot is



(a)



(b)

Figure 6.4: Virtual region selection behavior: The robot on the bottom left corner selects the center of the targets on the right as a goal position because there is the peak of the utility distribution. The utility distribution becomes balanced after the re-positioning.

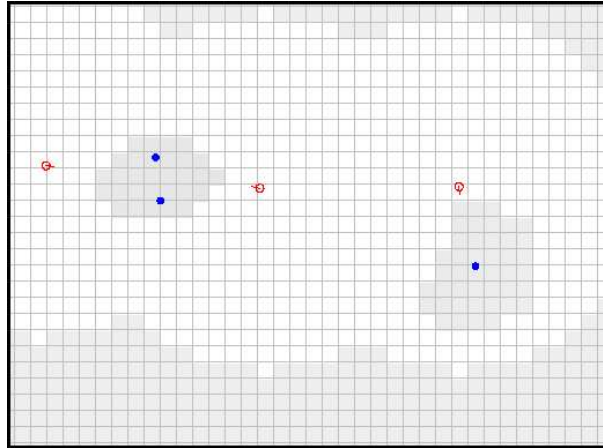
different from others, which is the reason why the left robot did not migrate to the right while the central one did.

6.4 Discussion

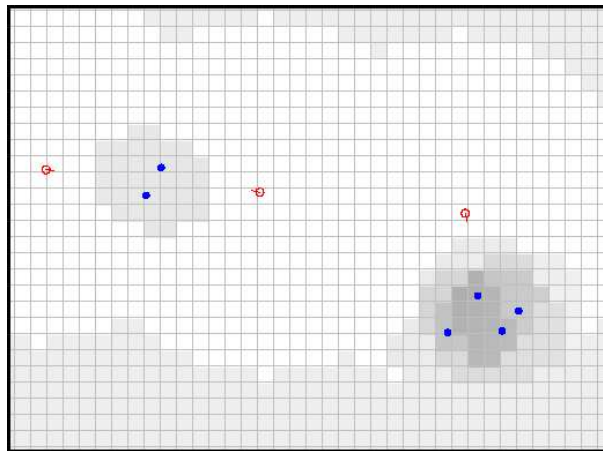
The *Grid Region-based Approach* was applied to the multiple moving objects tracking problem, and the study of utility distribution changes confirmed that robots were properly distributed according to the target distribution. One limitation of the current system is the lack of temporal memory. Since the algorithms does not 'remember' that a region was empty after a robot leaves

the region, it is possible that a robot may oscillate between two empty regions; however, by setting the cost function parameters of the VFH+ navigation algorithm properly, this worst case can be avoided.

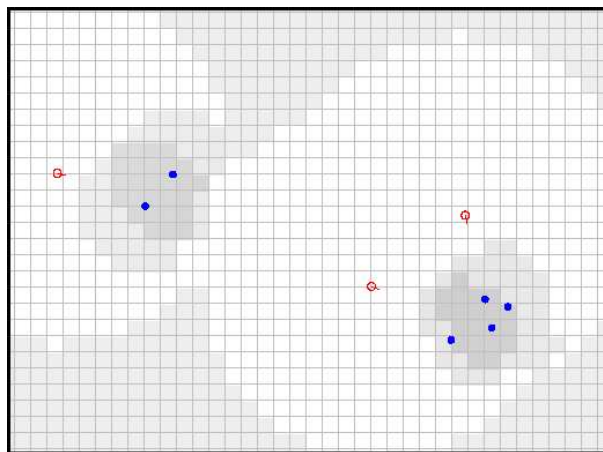
The effectiveness of the *Grid Region-based Approach* was validated by initial simulation results, but more intensive *experiments in simulation and with real robots* are expected in order to analyze the performance of the algorithm. We also plan *to investigate explicit exploration strategies* to control robot motion when it is available to move, and no urgent region needs servicing. The current system select a region randomly. By adopting a more sophisticated exploration strategy, performance enhancements can be expected.



(a)



(b)



(c)

Figure 6.5: Region-switching behavior: The robot in the center migrates to the right after the robot on the right discovers more targets. The utility distribution becomes balanced after the re-positioning.

Chapter 7

Conclusion and Future Work

In this thesis proposal we presented a solution for the multiple target tracking problem using multiple mobile robots. Our hierarchical approach decoupled the low-level, single-robot tracking algorithm and the high-level, multi-robot coordination strategy.

For single robot-based tracking, we presented the ego-motion compensation method using salient feature tracking and the adaptive particle filter to handle the noise and uncertainty of sensor inputs. The proposed method has been implemented and tested in various outdoor environments using three different robot platforms: a robotic helicopter, a Segway RMP, and a Pioneer2 AT, which have unique ego-motion characteristics. Measurements from a laser rangefinder were integrated into the tracking system by projecting them into an image space in order to achieve partial 3-dimensional estimates.

For multi-robot coordination, we presented the *Region-based Approach* treating the densities of robots and targets as properties of the environment in which they are embedded. The approach was described and validated through an example. Having observed that the general approach can be significantly improved in the special case where the topology of the environment is known in advance, we derived a specialized version of the control law for the structured environment case. This coarse discretization of the original method is called the *Topological Region-Based Approach*. We also gave the formulation of the solution in the unstructured case, and this fine discretization of the original method is called the *Grid Region-Based Approach*. These coordination approaches have been implemented in simulation, and in real robot systems. Experiments indicated that our treatment of the coordination problem based on environmental characteristics was effective and efficient.

7.1 Research Plan

Additional contributions to the work presented in this thesis proposal, which will be included in the final thesis, include:

1. Sensor fusion technique for partial 3D position estimation

As mentioned in Section 3.7, the position of a moving object in the image space is estimated independently from the distance information of a laser rangefinder. The current system integrates laser range scans into the estimation system by simply projecting the scans into the 2D image space, which causes poor estimation results when a robot turns at high velocity. There are two possible improvement for this unknown latency problem:

Task 1 Modify the current particle filter such that the measurement model embraces not only difference images but also projected range data.

Task 2 Add an additional probabilistic filter that takes the 2D estimates and range data as inputs, and estimates partial 3D position information.

Both approaches will be implemented, and their performance will be compared.

2. Performance analysis of the *Region-based Approach*

Task 3 The stability properties of the *Region-based Approach* will be analyzed theoretically and through simulations. The system's behavior in response to static or oscillating target motions will be studied.

Task 4 The performance of the *Grid Region-based Approach* will be tested and characterized through intensive simulations with various configurations in order to investigate the effect of environmental structure, broken inter-robot communication links, and increased target population.

3. Real-robot experiments in an outdoor environment

The *Grid Region-based Approach* has been tested thus far through a simple simulation (see Chapter 6). The entire tracking system will be tested thoroughly to validate the effectiveness of the proposed algorithm.

Task 5 All system components will be integrated and tracking experiments in an outdoor setting using multiple robots will be performed to test the robustness of the entire system.

Date	Mar	Apr	May	Jun	Jul	Aug	Sep	Oct	Nov	Dec	Jan 05
Task 1	■		■								
Task 2		■	■								
Task 3							■	■			
Task 4								■	■		
Task 5				■	■	■					
Task 6			■				■		■	■	■

Table 7.1: Timetable for future work

4. Writing dissertation

Task 6 The final dissertation will be written.

Table 7.1 shows my future research plan toward the completion of this thesis.

Bibliography

- Yaakov Bar-Shalom, editor. *Multitarget-Multisensor Tracking: Advanced Applications*. Artech House, 1990.
- Yaakov Bar-Shalom, editor. *Multitarget-Multisensor Tracking: Applications and Advances*, volume II. Artech House, Norwood, MA, 1992.
- Yaakov Bar-Shalom, K. C. Chang, and Henk A. P. Blom. Tracking a maneuvering target using input estimation versus the interacting multiple model algorithm. *IEEE Transactions on Aerospace and Electronic Systems*, AES-25(2):296–300, March 1989.
- Yaakov Bar-Shalom and Thomas E. Fortmann. *Tracking and Data Association*. Academic Press, Inc., Orlando, Florida, 1988.
- Alireza Behrad, Ali Shahrokni, and Seyed Ahmad Motamedi. A robust vision-based moving target detection and tracking system. In *the Proceeding of Image and Vision Computing Conference*, University of Otago, Dunedin, New Zealand, November 2001.
- George Biernson. *Optimal Radar Tracking Systems*. John Wiley & Sons, New York, 1990.
- Samuel S. Blackman. *Multiple Target Tracking with Radar Applications*. Artech House, Norwood, MA, 1986.
- Samuel S. Blackman. Association and fusion of multiple sensor data. In Yaakov Bar-Shalom, editor, *Multitarget-Multisensor Tracking: Advanced Applications*, chapter 6, pages 187–218. Artech House, 1990.
- Henk A. P. Blom and Yaakov Bar-Shalom. The interacting multiple model algorithm for systems with markovian switching coefficients. *IEEE Transactions on Automatic Control*, 33(8):780–783, August 1988.
- Philip L. Bogler. *Radar Principles with Applications to Tracking Systems*. John Wiley & Sons, New York, 1990.
- Jean-Yves Bouguet. Pyramidal implementation of the lucas kanadee feature tracker: Description of the algorithm. Technical report, Intel Research Laboratory, 1999.
- Ulisses Braga-Neto and John Goutsias. Automatic target detection and tracking in forward-looking infrared image sequences using morphological connected operators. In *Proceedings of the 23rd Conference on Information Sciences and Systems*, pages 173–178, Baltimore, Maryland, March 1999.

- Alex Brooks and Stefan Williams. Tracking people with networks of heterogeneous sensors. In *Proceedings of the Australasian Conference on Robotics and Automation*, Brisbane, Australia, December 2003.
- Jean-Pierre Le Cadre Carine Hue and Patrick Pérez. Sequential monte carlo methods for multiple target tracking and data fusion. *IEEE Transactions on Signal Processing*, 50(2):309–325, February 2002.
- Frederic Cazals and Mateu Sbert. Some integral geometry tools to estimate the complexity of 3d scenes. Technical Report RR-3204, Institut National de Recherche en Informatique et en Automatiue (INRIA), 1997.
- Alberto Censi, Andrea Fusiello, and Vito Roberto. Image stabilization by features tracking. In *Proceedings of the 10th International Conference on Image Analysis and Processing*, pages 665–667, Venice, Italy, September 1999.
- Chee-Yee Chong, Shozo Mori, and Kuo-Chu Chang. Distributed multitarget multisensor tracking. In Yaakov Bar-Shalom, editor, *Multitarget-Multisensor Tracking: Advanced Applications*, chapter 8, pages 247–295. Artech House, 1990.
- Howie Choset and Joel Burdick. Sensor based planning, part i: The generalized voronoi graph. In *Proceedings of the 1995 IEEE International Conference on Robotics and Automation*, volume 2, pages 1649–1655, Nagoya, Japan, may 1995a.
- Howie Choset and Joel Burdick. Sensor based planning, part ii: Incremental construction of the generalized voronoi graph. In *Proceedings of the 1995 IEEE International Conference on Robotics and Automation*, volume 2, pages 1643–1648, Nagoya, Japan, may 1995b.
- Jiyoon Chung and Hyun S. Yang. Fast and effective multiple moving targets tracking method for mobile robots. In *Proceedings of the 1995 IEEE International Conference on Robotics and Automation*, pages 2645–2650, 1995.
- Isaac Cohen and Gerard Medioni. Detecting and tracking objects in video surveillance. In *Proceeding of the IEEE Computer Vision and Pattern Recognition 99*, pages 319–325, Fort Collins, June 1999.
- Robert L. Cooperman. Tactical ballistic missile tracking using the interacting multiple model algorithm. In *Proceedings of the Fifth International Conference on Information Fusion*, pages 824–831, 2002.
- Christophe Coué and Pierre Bessière. Chasing an elusive target with a mobile robot. In *Proceedings of the 2001 IEEE/RSJ International Conference on Intelligent Robots and Systems*, pages 1370–1375, Maui, Hawaii, October 2001.
- Ingemar J. Cox and Sunita L. Hingorani. An efficient implementation of reid’s multiple hypothesis tracking algorithm and its evaluation for the purpose of visual tracking. *IEEE Transactions on Pattern Analysis and Machine Intelligence*, 18(2):138–150, February 1996.

- Martin P. Dana. Registration: A prerequisite for multiple sensor tracking. In Yaakov Bar-Shalom, editor, *Multitarget-Multisensor Tracking: Advanced Applications*, chapter 5, pages 155–185. Artech House, 1990.
- R. Danchick and G. E. Newnam. A fast method for finding the exact n-best hypotheses for multitarget tracking. *IEEE Transactions on Aerospace and Electronic Systems*, 29(2):555–560, April 1993.
- Goksel Dedeoglu, Maja J. Matarić, and Gaurav S. Sukhatme. Incremental, on-line topological map building with a mobile robot. In *Proceedings of Mobile Robots*, volume XIV, pages 129–139, Boston, MA, 1999.
- Goksel Dedeoglu and Gaurav S. Sukhatme. Landmark-based matching algorithm for cooperative mapping by autonomous robots. In *Distributed Autonomous Robotic Systems (DARS)*, pages 251–260, Knoxville, Tennessee, October 2000.
- David J. Difilippo and Lori L. Campbell. Design and implementation of a tracking algorithm for active missile approach warning systems. In *Proceedings of the Canadian Conference on Electrical and Computer Engineering*, pages 756–759, 1995.
- P. Fabiani, Héctor González-Baños, Jean-Claude Latombe, and David Lin. Tracking an unpredictable target among occluding obstacles under localization uncertainties. *Robotics and Autonomous Systems*, 38:31–48, 2002.
- Ajo Fod, Andrew Howard, and Maja J. Matarć. Laser-based people tracking. In *Proceedings of the IEEE International Conference on Robotics and Automation*, pages 3024–3029, Washington DC, May 2002.
- Gian Luca Foresti and C. Micheloni. A robust feature tracker for active surveillance of outdoor scenes. *Electronic Letters on Computer Vision and Image Analysis*, 1(1):21–34, 2003.
- David A. Forsyth and Jean Ponce. *Computer Vision: A Modern Approach*. Prentice Hall, 2003.
- Thomas E. Fortmann, Yaakov Bar-Shalom, and Molly Scheffe. Sonar tracking of multiple targets using joint probabilistic data association. *IEEE Journal of Oceanic Engineering*, OE-8(3): 173–184, July 1983.
- Dieter Fox. KLD-sampling: Adaptive particle filter. In *Advances in Neural Information Processing Systems 14*. MIT Press, 2001.
- Oliver Frank. *Multiple Target Tracking*. PhD thesis, Swiss Federal Institute of Technology Zurich, February 2003.
- Brian Gerkey and Maja J Matarić. Principled communication for dynamic multi-robot task allocation. In D. Rus and S. Singh, editors, *Experimental Robotics*, volume LNCIS 271 of VII, pages 353–362, Springer-Verlag Berlin Heidelberg, 2001.
- Brian Gerkey, Richard Vaughan, Kasper Stoy, Andrew Howard, Gaurav S. Sukhatme, and Maja J Matarić. Most valuable player: A robot device server for distributed control. In *Proceedings of the IEEE/RSJ International Conference on Intelligent Robots and Systems*, pages 1226–1231, Wailea, Hawaii, October 2001.

- Leonidas J. Guibas. Sensing, tracking, and reasoning with relations. *IEEE Signal Processing Magazine*, March 2002.
- Leonidas J. Guibas, Jean-Claude Latombe, Steven M. LaValle, David Lin, and Rajeev Motwani. A visibility-based pursuit-evasion problem. *International Journal of Computational Geometry and Applications*, 9(5):471–494, October 1997.
- Fedrik Gustafsson, Fedrik Gunnarsson, Kiclas Bergman, Urban Forssell, Jonas Jansson, Rickard Karlsson, and Per-Johan Nordlund. Particle filters for positioning, navigation, and tracking. *IEEE Transactions on Signal Processing*, 50(2):425–437, February 2002.
- Ismail Haritaoglu, David Harwood, and Larry S. Davis. w^4s : A real-time system for detecting and tracking people in $2\frac{1}{2}d$. In *Proceeding of the European Conference on Computer Vision*, pages 877–892, 1998.
- Trevor Hastie, Robert Tibshirani, and Jerome Friedman. *The Elements of Statistical Learning: Data Mining, Inference, and Prediction*. Springer, 2001.
- Shawn M. Herman. *A Particle Filtering Approach to Joint Passive RADAR Tracking and Target Classification*. PhD thesis, University of Illinois at Urbana-Champaign, Urbana, Illinois, 2002.
- Brian Horling, Regis Vincent, Roger Mailler, Jiaying Shen, Raphen Becker, Kyle Rawlins, and Victor Lesser. Distributed sensor network for real time tracking. In *Proceedings of the 5th International Conference on Autonomous Agents*, pages 417–424, 2001.
- A. Houles and Y. Bar-Shalom. Multisensor tracking of a maneuvering target in clutter. *IEEE Transactions on Aerospace and Electronic Systems*, AES-25(2):176–189, March 1989.
- Andrew Howard, Maja Matarić, and Gaurav Sukhatme. Relaxation on a mesh: a formalism for generalized localization. In *Proceedings of the IEEE/RSJ International Conference on Intelligent Robots and Systems*, pages 1055–1060, Wailea, Hawaii, October 2001.
- Carine Hue, Jean-Pierre Le Cadre, and Patrick Pérez. A particle filter to track multiple objects. In *IEEE Workshop on Multi-Object Tracking*, pages 61–68, Vancouver, Canada, July 2001.
- Norikazu Ikoma, Tomoyuki Higuchi, and Hiroshi Maeda. Maneuvering target tracking by using particle filter method with model switching structure. In *Proceedings of the Conference for Computational Statistics*, Berlin, Germany, August 2002.
- Michal Irani, Renny Rousso, and Shmuel Peleg. Recovery of ego-motion using image stabilization. In *Proceedings of the IEEE Computer Vision and Pattern Recognition*, pages 454–460, March 1994.
- Michael Isard and Andrew Blake. Condensation – conditional density propagation for visual tracking. *International Journal of Computer Vision*, 29(1):5–28, 1998.
- Simon J. Julier and Jeffrey K. Uhlmann. A new extension of the kalman filter to nonlinear systems. In *Proceedings of AeroSense: The 11th International Symposium on Aerospace/Defence Sensing, Simulation and Controls*, pages 182–193, Orlando, Florida, 1997.

- Boyoon Jung and Gaurav S. Sukhatme. Tracking multiple moving targets using a camera and laser rangefinder. Institute for Robotics and Intelligent Systems Technical Report IRIS-01-397, University of Southern California, 2001.
- Boyoon Jung and Gaurav S. Sukhatme. Tracking targets using multiple robots: The effect of environment occlusion. *Autonomous Robots*, 13(3):191–205, 2002.
- Boyoon Jung and Gaurav S. Sukhatme. Detecting moving objects using a single camera on a mobile robot in an outdoor environment. In *International Conference on Intelligent Autonomous Systems*, The Netherlands, March 2004.
- Jinman Kang, Isaac Cohen, and Gerard Medioni. Continuous multi-views tracking using tensor voting. In *Proceedings of the IEEE Workshop on Motion and Video Computing*, pages 181–186, Orlando, Florida, December 2002.
- Jinman Kang, Isaac Cohen, and Gerard Medioni. Continuous tracking within and across camera streams. In *Proceedings of the IEEE Computer Society Conference on Computer Vision and Pattern Recognition*, pages 267–272, Madison, Wisconsin, June 2003.
- Thiagalingam Kirubarajan, Yaakov Bar-Shalom, and Yueyong Wang. Passive ranging of a low observable ballistic missile in a gravitational field. *IEEE Transactions on Aerospace and Electronic Systems*, 37(2):481–494, April 2001.
- Boris Kluge, Christian Kohler, and Erwin Prassler. Fast and robust tracking of multiple moving objects with a laser range finder. In *Proceedings of the 2001 IEEE International Conference on Robotics and Automation*, pages 1683–1688, 2001.
- Michael O. Kolawole. *Radar Systems, Peak Detection and Tracking*. Newnes, Burlington, MA, 2002.
- Hiroshi Koyasu, Jun Miura, and Yoshiaki Shirai. Realtime omnidirectional stereo for obstacle detection and tracking in dynamic environments. In *Proceedings of the 2001 IEEE/RSJ International Conference on Intelligent Robots and Systems*, pages 31–36, Maui, Hawaii, October 2001.
- Benjamin Kuipers and Young-Tai Byun. A robot exploration and mapping strategy based on a semantic hierarchy of spatial representations. *Journal of Robotics and Autonomous Systems*, 8:47–63, 1991.
- Clayton Kunz, Tomas Willeke, and Illah R. Nourbakhsh. Automatic mapping of dynamic office environments. *Autonomous Robots*, 7(2), February 1999.
- Steven M. LaValle, Héctor González-Baños, Craig Becker, and Jean-Claude Latombe. Motion strategies for maintaining visibility of a moving target. In *Proceedings of the 1997 IEEE International Conference on Robotics and Automation*, 1997.
- Dan Li, Kerry D. Wong, Yu H. Hu, and Akbar M. Sayeed. Detection, classification and tracking of targets in distributed sensor networks. *IEEE Signal Processing Magazine*, 19(2):17–29, March 2002.

- Alan J. Lipton, Hironobu Fujiyoshi, and Raju S. Patil. Moving target classification and tracking from real-time video. In *Proceeding of the IEEE Workshop on Applications of Computer Vision*, pages 8–14, Princeton NJ, October 1998.
- David Liu and Li-Chen Fu. Target tracking in an environment of nearly stationary and biased clutter. In *Proceedings of the 2001 IEEE/RSJ International Conference on Intelligent Robots and Systems*, pages 1358–1363, Maui, Hawaii, October 2001.
- Jie Liu, Patrick Cheung, Leonidas Guibas, and Feng Zhao. A dual-space approach to tracking and sensor management in wireless sensor networks. Technical Report P2002-10077, Palo Alto Research Center, March 2002.
- Bruce D. Lucas and Takeo Kanade. An iterative image registration technique with an application to stereo vision. In *Proceedings of the 7th International Joint Conference on Artificial Intelligence*, pages 674–697, 1981.
- Maja J. Matarić. Behavior-based control: Examples from navigation, learning, and group behavior. *Journal of Experimental and Theoretical Artificial Intelligence, special issue on Software Architectures for Physical Agents*, 9(2-3):67–83, 1997.
- Peter S. Maybeck, Theodore D. Herrera, and Roger J. Evans. Target tracking using infrared measurements and laser illumination. *IEEE Transactions on Aerospace and Electronic Systems*, 30(3):758–768, July 1994.
- E. Mazor, A. Averbuch, Y. Bar-Shalom, and J. Dayan. Interacting multiple model methods in target tracking: A survey. *IEEE Transactions on Aerospace and Electronic Systems*, 34(1):103–123, January 1998.
- Shaun McGinnity and George W. Irwin. Manoeuvring target tracking using a multiple-model bootstrap filter. In Arnaud Doucet, Nando de Freitas, and Neil Gordon, editors, *Sequential Monte Carlo Methods in Practice*, chapter 23, pages 479–497. Springer, 2001.
- Esther B. Meier and Frank Ade. Using the condensation algorithm to implement tracking for mobile robots. In *Proceedings of the Third European Workshop on Advanced Mobile Robots*, pages 73–80, 1999.
- Michael Montemerlo, Sebastian Thrun, and William Whittaker. Conditional particle filters for simultaneous mobile robot localization and people-tracking. In *Proceedings of the IEEE International Conference on Robotics and Automation*, pages 695–701, Washington DC, May 2002.
- Jamila Moore, Thomas Keiser, Richard Brooks, Shashi Phoha, David Friedlander, John Koch, and Noah Jacobson. Tracking targets with self-organizing distributed ground sensors. In *Proceedings of IEEE Aerospace Conference*, pages 5_2113–5_2123, March 2003.
- Don Murray and Anup Basu. Motion tracking with an active camera. *IEEE Transactions on Pattern Analysis and Machine Intelligence*, 16(5):449–459, May 1994.

- Rafael Murrieta-Cid, Héctor González-Baños, and Benjamín Tovar. A reactive motion planner to maintain visibility of unpredictable targets. In *the Proceeding of IEEE International Conference on Robotics and Automation*, pages 4242–4247, Washington DC, May 2002.
- Keiji Nagatani and Howie Choset. Toward robust sensor based exploration by constructing reduced generalized voronoi graph. In *Proceedings of the 1999 IEEE/RSJ International Conference on Intelligent Robots and Systems*, volume 3, pages 1687–1692, October 1999.
- Peter Nordlund and Tomas Uhlin. Closing the loop: Detection and pursuit of a moving object by a moving observer. *Image and Vision Computing*, 14:265–275, May 1996.
- Matthew Orton and William Fitzgerald. A bayesian approach to tracking multiple targets using sensor arrays and particle filters. *IEEE Transactions on Signal Processing*, 50(2):216–223, February 2002.
- Lynne E. Parker. Cooperative motion control for multi-target observation. In *Proceedings of the 1997 IEEE/RSJ International Conference on Intelligent Robots and Systems*, pages 1591–1598, 1997.
- Lynne E. Parker. Cooperative robotics for multi-target observation. *Intelligent Automation and Soft Computing, special issue on Robotics Research at Oak Ridge National Laboratory*, 5(1): 5–19, 1999.
- Donald B. Reid. An algorithm for tracking multiple targets. *IEEE Transactions on Automatic Control*, AC-24(6):843–854, December 1979.
- Ioannis Rekleitis, Robert Sim, Gregory Dudek, and Evangelos Miliotis. Collaborative exploration for the construction of visual maps. In *Proceedings of the 2001 IEEE/RSJ International Conference on Intelligent Robots and Systems*, pages 1269–1274, Maui, Hawaii, October 2001.
- Srikanth Saripalli, James F. Montgomery, and Gaurav S. Sukhatme. Visually-guided landing of an unmanned aerial vehicle. *IEEE Transactions on Robotics and Automation*, 19(3):371–381, Jun 2003.
- Dirk Schultz, Wolfram Burgard, Dieter Fox, and Armin B. Cremers. Tracking multiple moving targets with a mobile robot using particle filters and statistical data association. In *Proceedings of the 2001 IEEE International Conference on Robotics and Automation*, pages 1165–1170, 2001.
- George M. Siouris, Guanrong Chen, and Jianrong Wang. Tracking an incoming ballistic missile using an extended interval kalman filter. *IEEE Transactions on Aerospace and Electronic Systems*, 33(1):232–240, January 1997.
- Taek L. Song, Jo Young Ahn, and Tae Yoon Um. A passive tracking filter for missile capture. *IEEE Transactions on Aerospace and Electronic Systems*, 26(5):867–875, September 1990.
- John R. Spletzer and Camillo J. Taylor. Dynamic sensor planning and control for optimally tracking targets. *International Journal of Robotics Research (IJRR)*, 22(1):7–20, January 2003.

- Sridhar Srinivasan and Rama Chellappa. Image stabilization and mosaicking using the overlapped basis optical flow field. In *Proceedings of IEEE International Conference on Image Processing*, pages 356–359, October 1997.
- Scott Stillman, Rawesak Tanawongsuwan, and Irfan Essa. A system for tracking and recognizing multiple people with multiple cameras. Technical Report GIT-GVU-98-25, Georgia Institute of Technology, Graphics, Visualization and Usability Center, August 1998.
- Ashley W. Stroupe, Martin C. Martin, and Tucker Balch. Distributed sensor fusion for object position estimation by multi-robot systems. In *Proceedings of the IEEE International Conference on Robotics and Automation*, pages 1092–1098, May 2001.
- Sebastian Thrun, Dieter Fox, Wolfram Burgard, and Frank Dellaert. Robust monte carlo localization for mobile robots. *Artificial Intelligence*, 128:99–141, 2001.
- Carlo Tomasi and Takeo Kanade. Detection and tracking of point features. Technical Report CMU-CS-91-132, Carnegie Mellon University, Pittsburgh, PA, April 1991.
- Nicola Tomatis, Illah Nourbakhsh, and Roland Siegwart. Simultaneous localization and map building: A global topological model with local metric maps. In *Proceedings of the 2001 IEEE/RSJ International Conference on Intelligent Robots and Systems*, pages 421–426, Maui, Hawaii, October 2001.
- Iwan Ulrich and Johann Borenstein. VFH+: Reliable obstacle avoidance for fast mobile robots. In *Proceeding of the IEEE International Conference on Robotics and Automation*, pages 1572–1577, Leuven, Belgium, May 16–21 1998.
- P. Vacher, I. Barret, and M. Gauthier. Design of a tracking algorithm for an advanced atc system. In Yaakov Bar-Shalom, editor, *Multitarget-Multisensor Tracking: Applications and Advances*, volume II, chapter 1, pages 1–29. Artech House, 1992.
- Marinus B. van Leeuwen and Frans C.A. Groen. Motion interpretation for in-car vision systems. In *Proceedings of the IEEE/RSJ International Conference on Intelligent Robots and Systems*, pages 135–140, EPFL, Lausanne, Switzerland, October 2002.
- Richard T. Vaughan. Stage: A multiple robot simulator. Institute for Robotics and Intelligent Systems Technical Report IRIS-00-393, University of Southern California, 2000.
- Greg Welch and Gary Bishop. An introduction to the kalman filter. Technical Report 95-041, Department of Computer Science, University of North Carolina at Chapel Hill.
- Barry B. Werger and Maja J. Matarić. Broadcast of local eligibility for multi-target observation. In *Proceedings of Distributed Autonomous Robotic Systems*, pages 347–356, 2000.
- T. Wilhelm, H. J. Böhme, and H. M. Gross. Sensor fusion for vision and sonar based people tracking on a mobile service robot. In *Proceedings of the International Workshop on Dynamic Perception*, pages 315–320, 2002.
- Yingqi Xu and Wang-Chien Lee. On localized prediction for power efficient object tracking in sensor networks. In *Proceedings of the 23rd International Conference on Distributed Computing Systems Workshops*, pages 434–439, Providence, Rhode Island, May 2003.

- Masfumi Yamashita, Hideki Umemoto, Ichiro Suzuki, and Tsunehiko Kameda. Searching for mobile intruders in a polygonal region by a group of mobile searchers. In *Symposium on Computational Geometry*, pages 448–450, 1997.
- Alper Yilmaz, Khurram Shafique, Niels Lobo, Xin Li, Teresa Olson, and Mubarak a. Shah. Target-tracking in flir imagery using mean-shift and global motion compensation. In *Workshop on Computer Vision Beyond the Visible Spectrum*, Kauai, Hawaii, December 2001.
- Wensheng Zhang and Guohong Cao. Optimizing tree reconfiguration for mobile target tracking in sensor networks. In *Proceedings of the IEEE International Conference on Computer Communication (INFOCOM)*, March 2004.
- Feng Zhao, Jaewon Shin, and James Reich. Information-driven dynamic sensor collaboration for tracking applications. *IEEE Signal Processing Magazine*, 19(2):61–72, March 2002.
- I. Zoghlami, O. Faugeras, and R. Deriche. Using geometric corners to build a 2d mosaic from a set of images. In *Proceedings of the IEEE Conference on Computer Vision and Pattern Recognition*, pages 420–425, 1997.

Appendix A

List of Publications

Summary: 2 refereed journal paper, 7 conference papers (5 appeared, 1 accepted, 1 submitted), and 4 unrefereed publications (technical reports).

A.1 Refereed Journal Papers

1. Boyoon Jung and Gaurav S. Sukhatme, "Tracking Targets using Multiple Robots: The Effect of Environment Occlusion," In *Autonomous Robots*, Vol. 13, No. 3, pp. 191-205, Nov 2002.
2. Boyoon Jung and Kyung-Hwan Oh, "An Automatic Cooperative Coordination Model for the Multi-Agent System using Reinforcement Learning," In *Korean Journal of Cognitive Science*, February, 1999.

A.2 Refereed Conference Papers

1. Boyoon Jung and Gaurav S. Sukhatme, "A Generalized Region-based Approach for Multi-target Tracking in Outdoor Environments," To appear in *Proceedings of the IEEE International Conference on Robotics and Automation*, New Orleans, LA, April 2004.
2. Boyoon Jung and Gaurav S. Sukhatme, "Detecting Moving Objects using a Single Camera on a Mobile Robot in an Outdoor Environment," To appear in *Proceedings of the International Conference on Intelligent Autonomous Systems*, Amsterdam, The Netherlands, Mar 2004.
3. Boyoon Jung and Gaurav S. Sukhatme, "A Region-based Approach for Cooperative Multi-Target Tracking in a Structured Environment," In *Proceedings of the IEEE/RSJ International Conference on Intelligent Robots and Systems*, pp. 2764-2769, EPFL, Switzerland, Oct 2002.
4. Milo Silverman, Dan M. Nies, Boyoon Jung, and Gaurav S. Sukhatme, "Staying Alive: A Docking Station for Autonomous Robot Recharging," In *Proceedings of the IEEE International Conference on Robotics and Automation*, pp. 1050-1055, Washington D.C., May 2002.

5. Boyoon Jung and Gaurav S. Sukhatme, "Cooperative Tracking using Mobile Robots and Environment-Embedded, Networked Sensors," In *Proceedings of the International Symposium on Computational Intelligence in Robotics and Automation*, pp. 206-211, Banff, Alberta, Canada, Jul 2001.
6. Ambrish Verma, Boyoon Jung, and Gaurav S. Sukhatme, "Robot Box-Pushing with Environment-Embedded Sensor," In *Proceedings of the International Symposium on Computational Intelligence in Robotics and Automation*, pp. 212-217, Banff, Alberta, Canada, Jul 2001.
7. Boyoon Jung and Kyung-Hwan Oh, "Role Assignment and Coordination Model for Mobile Agent Cooperation," in *Proceeding of HCI Conference*, Korea Information Science Society, February 1998.

A.3 Unrefereed Technical Reports

1. Milo Silverman, Boyoon Jung, Dan M. Nies, and Gaurav S. Sukhatme, "Staying Alive Longer: Autonomous Robot Recharging Put to the Test," *Center for Robotics and Embedded Systems Technical Report*, CRES-03-015, University of Southern California, 2003.
2. Boyoon Jung and Gaurav S. Sukhatme, "Tracking Anonymous Targets using a Robotics Sensor Network," *The 2002 AAI Spring Symposium Technical Report*, SS-02-04, AAI Press, 2002.
3. Boyoon Jung and Gaurav S. Sukhatme, "Tracking Multiple Moving Targets using a Camera and Laser Rangefinder," *Institute for Robotics and Intelligent Systems Technical Report*, IRIS-01-397, University of Southern California, 2001.
4. Boyoon Jung and Gaurav S. Sukhatme, "Cooperative Tracking with Mobile Robots and Networked Embedded Sensors," *Institute for Robotics and Intelligent Systems Technical Report*, IRIS-01-404, University of Southern California, 2001.

Appendix B

Extension: Visibility Maximization

The *Region-based Approach* is able to adopt other indicators as well. The approach described in Section 4.5 might be improved by using visibility (LaValle et al., 1997) instead of the robot density. The region-based approach using the robot and target densities does not always maximize the total coverage in a region; for example, if the sensor ranges of robots in a region overlap, the total coverage within the region is often small even though there are enough robots in the region. In order to obtain a good robot spread within a region, a visibility maximization method is used. The visibility of a region R is defined as:

$$Visibility(R) = \frac{\text{the covered area of region } R}{\text{area of region } R} \quad (\text{B.1})$$

Calculating an accurate covered area of each region requires a single, unified global coordinate system and geometrical information of all robots in it. This is unrealistic in dynamic environments and does not scale. In addition, every computation needs to be done in real-time. Therefore, the covered area should be estimated with given imperfect information. The system performance is expected to depend on the accuracy of the visibility estimation. In our system, the estimation process consists of two steps: *coverage assignment* and *overlap subtraction*.

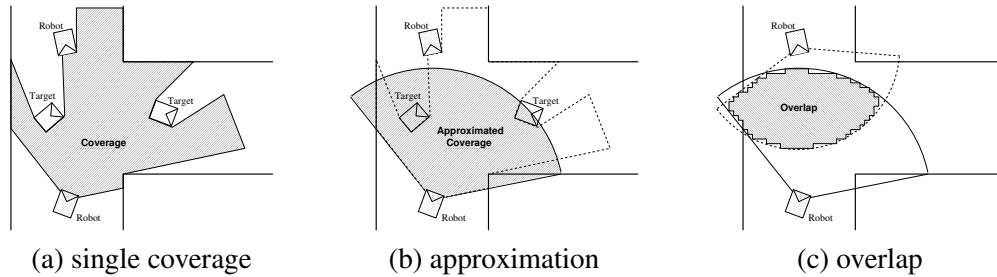


Figure B.1: Coverage computation: The coverage of a single robot is computed by integrating the distance readings, and the total coverage of all robots is the sum of each coverage. For more accurate computation, overlap is subtracted from the result.

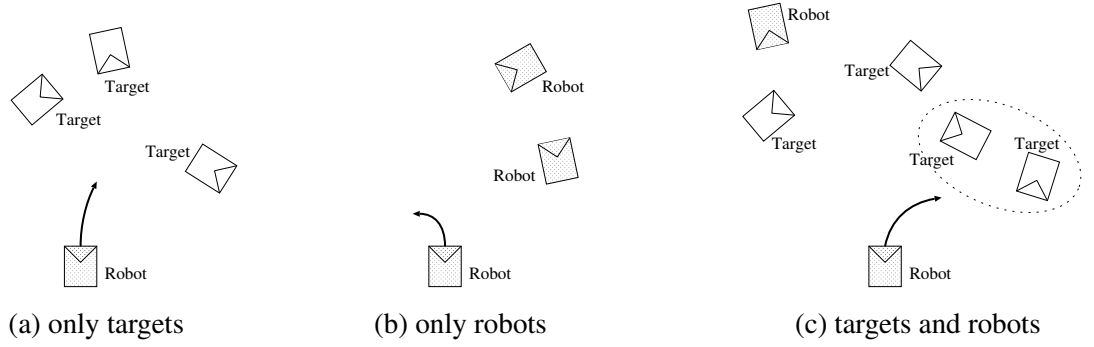


Figure B.2: Visibility maximization method relying on local sensing: A robot decides its behavior based on a local situation; therefore, explicit communication or negotiation is not required.

Step 1: Coverage Allocation The coverage of a robot r is computed by integrating the distance function $l_r(\theta)$ of its laser rangefinder in the FOV of its camera (Figure B.1 (a)).

$$coverage(r) = \int_0^{FOV} \frac{1}{2} l_r^2(\theta) d\theta \quad (B.2)$$

Once the coverage of each robot has been computed, it is assigned to regions based on the current robot position. When a robot is positioned in the middle of multiple regions, the coverage is divided and assigned to those regions evenly.

Step 2: Overlap Subtraction For real-time computation, overlapping coverage is checked only between robots in the same region, and the coverage of each robot is approximated as a single sector with a radius of the average distance of laser readings (Figure B.1 (b)). The overlapping coverage between two sectors is subtracted from the total coverage (Figure B.1 (c)) since it has been counted twice.

For the coarse deployment strategy, the robot density $D_r(R)$ is simply replaced with $Visibility(R)$, and the rest of the strategy remains the same as described in Section 4.5.2. However, the movement within a region is modified in order to pursue two goals in parallel; each robot tries to maximize the number of targets tracked, and to maximize the coverage of regions.

Maximizing coverage implies reducing the overlap of robots' coverage, so robots should keep maximum distance from each other. We use the following method relying on only local sensing and computation.

1. If there are only targets in its sensing range as shown in Figure B.2 (a), a robot tracks the group of targets as described in Section 4.5.3.

2. If there are only robots in its sensing range as shown Figure B.2 (b), a robot turns in a direction opposite to the group of robots.
3. If there are both targets and robots in its sensing range as shown in Figure B.2 (c), a robot tracks only the group of targets which are closer to itself, and assumes that the rest of them would be tracked by the other robots.

The advantage of this method is that it does not require explicit communication or negotiation among robots.